BEHAVIOR OF L-SHAPED REINFORCED CONCRETE COLUMNS UNDER COMBINED BIAXIAL BENDING AND COMPRESSION

by

Amar Shah

Thesis submitted to the Faculty of the Graduate School of the New Jersey Institute of Technology in partial fulfillment of the requirement for the degree of Master of Science in Civil Engineering
1984

APPROVAL SHEET

Title of Thesis : Behavior of L-shaped Reinforced Concrete Columns under Combined Biaxial Bending and Compression

Name of Candidate : Amar Shah
Master of Science in Civil Engineering

Thesis and Abstact Approved :

______________________ 5/11/84
Date

C. T. Thomas Hsu, PhD.
Associate Professor,
Department of Civil and Environmental Engineering

Signatures of other members of the thesis committee :

______________________ 5/11/84
Date

______________________ 5/11/84
Date

VITA

Name : Amar Shah

Degree and date to be conferred : MSCE, 1984.

Secondary education : C. N. Vidhyalaya, India,
June 1975.

Collegiate institutions attended	Date	Degree	Date of Degree
L. D. College of Engineering, India	6/77-6/81	BSCE	Aug. 1981
New Jersey Institute of Technology, Newark N. J., U. S. A.	9/82-5/84	MSCE	May 1984

Major : Civil Engineering.

ABSTRACT

Title of Thesis :	Behavior of L-shaped Reinforced Concrete Columns under Combined Biaxial Bending and Compression.
Amar Shah,	Master of Science in Civil Engineering, 1984
Thesis directed by :	Dr. C. T. Thomas Hsu, Associate Professor of Civil Engineering.

Combined biaxial and axial compression for L-shaped reinforced concrete short columns is a common design problem. Current code provisions and the available design aids do not offer an insight into the determination of strength and ductility of biaxially loaded reinforced concrete column. An experimental and analytical investigation of the moment-deformation behavior of biaxially loaded L-shaped short columns were undertaken. Four 1/2 scaled specimens were tested till failure. Moment-curvature and load-deflection curves were developed from the experimental and the analytical results. The analytical results were obtained using a computer program developed by Hsu(1). From the investigation it is deduced that the computer program developed by Hsu(1) can be used to find the ultimate strength, the moment-deformation

characteristics, the stress and the strain distributions across the section of L-shaped, biaxially loaded column with large and small eccentricities.

To
my Parents and Krupa

ACKNOWLEDGEMENTS

I wish to thank Dr. C. T. Thomas Hsu for his valuable assistance and guidance throughout the entire project.

The participation of Mr. Parthasarthy Iyenger, Mr. Ramesh Damodaram, Mr. Anand Jagani, Mr. Ramanand Shetty, and Mr. Shenqkwang Jou during the casting and testing is greatfully appreciated.

I also thank Dr. Methi Wecheratana as well as my friends Mr. Subhash Yalamarthy and Mr. Tony Nader for their cooperation and good suggestions during the project.

TABLE OF CONTENTS

LIST OF FIGURES

LIST OF TABLES

LIST OF NOTATIONS

a_k - Area of element K

e_x - Eccentricity along X axis

e_y - Eccentricity along Y axis

$\mathcal{E}_c$ - Maximum Compressive Strain in Concrete

E_k - Strain in element K

E_s - Young's Modulus of elasticity for steel

f'_c - Ultimate strength of concrete

K - Element number

K_d - distance from maximum compressive concrete strain to the neutral axis

l - total length of column

l' - Effective length of column

M_{nx} - $P_n e_y$

M_{ny} - $P_n e_x$

M_{ox} - M_{nx} capacity at axial load P_n when M_y is zero

M_{oy} - M_{ny} capacity at axial load P_n when M_x is zero

M_{ult} - moment at failure

M_x - bending moment about X-axis

M_y - bending moment about Y-axis

P - axial load

s - spacing of lateral reinforcement

Ø - Curvature

LIST OF NOTATIONS (Continued)

ϕ_x - Curvature produced due to bending moment M_x

ϕ_y - Curvature produced due to bending moment M_y

δ_x - deflection in X-direction

δ_y - deflection in Y-direction

N_u - Ultimate normal force

ε_s - Strain in reinforcing steel

CHAPTER I

GENERAL INTRODUCTION AND SCOPE OF RESEARCH

A. GENERAL INTRODUCTION

Structural members subjected to axial load and biaxial bending are encountered in design practice from time to time; a typical example is the corner column in a framed structure. In recent years the idea of using irregularly shaped column (eg. L-shaped column) at corner of the framed structure and at enclosure of elevator shaft has drawn the attention of investigators.

Unfortunately, little is known about the analytical and experimental behavior of irregularly shaped columns subjected to combined biaxial bending and axial compression; further, most investigations into the behavior of columns under combined biaxial bending and axial compression states have been primarily concerned with the determination of the ultimate strength of concrete and relatively few studies have been made of deformational characteristics of concrete columns subjected to biaxial bending and axial compression.

It is felt that current code provisions and avialable methods do not offer an insight into the determination of strength and ductility of biaxially loaded reinforced concrete columns. This study lays a special emphasis on L-shaped columns, as the use of such columns can be expected to increase in future. To design such structural members the following provisions are needed:

1. Design aids such as interaction diagrams or modified load contour design equations for cross section other than rectangular or circular, from which computer models can be developed.

2. Verification of mathematical modelling transcribed into computer programs by experimental testing.

3. The stress strain relationship of concrete and reinforcing steel must be reexamined in its application to columns other than of standard shapes.

4. Load-deflection characteristics must be studied and mathematical equations should be proposed.

5. In addition to these, the moment-curvature

characteristics at every stage of loading would also be helpful to understand the complete behavior of the structural member.

B. RESEARCH OBJECTIVE

The investigation described here was carried out to find the possible answers of some of the above problems. The primary objective of this project is to study the strength and deformational behavior of L-shaped column under combined biaxial bending and axial compression experimentally, and to assess the accuracy of a computer program developed by Hsu(1) on the basis of equlibrium of forces based on input material stress-strain curves and strain compatibility. A modified Newton-Raphson numerical method was used to achieve computation procedure for Hsu's computer program.

The experimental result will form a basis for a recommended analysis and design technique. For experimental purpose four reinforced concrete columns were tested. Moment-curvature relationships are derived from these experimental results and compared with those obtained by using a computer program developed by Hsu(1).

C. DESIGN CRITERIA AND PRACTICE

The extensive research work done by many investigators has made it possible to develop different design criteria for eccentrically loaded columns such as working stress design, ultimate strength design, and limit design. Early recognition that compression limit at the extreme fibers of concrete cross sections produced unacceptably low estimates of allowable load preceded the adoption of a strength formulation of an allowable stress for the design of non-slender columns.

The present ACI Building Code (ACI 318-83)(9) and design aids follow the strength criteria as a basis for designing concrete columns in which failure is defined in terms of a limiting strain or stress in the concrete and the reinforcing steel. In the above criteria, the stress distribution in the compression zone of a section is defined in terms of the stress block parameters K_1, K_2, K_3 where these parameters are determined experimentally. According to ACI K_1=0.85, K_2 =0.5, K_3=0.85 for certain values of f_c' & f_y .

The methods available for the design of biaxially loaded columns are: (1) Trial and error procedure and (2) Determination of ultimate loads from failure surfaces in columns. The former method essentially involves a trial and error procedure for obtaining the position of an inclined neutral axis, hence this method is quite complex so that no formula can be easily developed for practical use. The concept of using failure surfaces has been presenterd by Bresler(12) and Pannel(13). Pannel(13) has shown that equivalent uniaxial moment M_{uxo} of the radial moment M_u corresponding to any ultimate load P_u can be determined with the aid of the parameter N, the deviation factor and the ratio of M_{ux}/M_{uy}. The calculated uni-axial moment is then determined from the major axis inter action diagrams. This procedure, namely, determining the load from the moments, is likely to give rise to possible errors in the estimation of the ultimate load, especially when failure is controlled by tension. Bresler proposed two approaches. Of these, the Load-contour method gives the general nondimensional equation at constant P as follows:

$$\left[\frac{M_{nx}}{M_{ox}}\right]^{\alpha_1} + \left[\frac{M_{ny}}{M_{oy}}\right]^{\alpha_2} = 1 \qquad \text{.........(1.1)}$$

Where, $M_{nx} = P_n e_y$; $M_{ny} = P_n e_x$

$M_{ox} = M_{nx}$ capacity at axial load P_n when M_{ny} (or e_y) is zero.

$M_{oy} = M_{ny}$ capacity at axial load P_n when M_{nx} (or e_x) is zero.

Bresler(12) suggested that it is acceptable to take $\alpha_1 = \alpha_2 = \alpha$ and reported the calculated values of α to vary from 1.15 to 1.55. Bresler(12) suggested another simple equation using the reciprocal method which is :

$$\frac{1}{P_i} = \frac{1}{P_{ux}} + \frac{1}{P_{uy}} + \frac{1}{P_o} \qquad \text{.........(1.2)}$$

This equation gives surprisingly satisfactory results.

A modification of extended Newton-Raphson method or method of successive approximation has been used by investigators for determination of strain and curvature distributions at reinforced concrete section of column under biaxial bending and axial load. Under this method the typical definition of failure was suggested by Cranston(19) who considered that if the maximum strains in the concrete or steel reinforcement exceed certain predefined maximum values, the section is considered to have failed. Hsu and Mirza(21) modified and extended Cranston's(19) numerical approach and the stress-strain curves to include the descending branch of the concrete stress-strain curve and developed a computer program which is used in this study. This program uses the material property of the concrete and reinforcing steel and the section geometry as an input features. The idealization of the stress-strain curve of the steel was done by piece-wise linear approximation. The out-put features of the program include moment-curvature behavior of a structural member under biaxial bending and compression. This program was compared with rectangular column tests by Anderson and Lee(23), Bresler(12), Ramamurthy(14) and Hsu(1). Excellent agreement was obtained between experimental and analytical results according to Hsu(1).

Design aids for L-shaped columns have been developed by Marin(2). Marin(2) presented three sample design charts from group of 50 to be published.

Recently Ramamurthy and Khan(22) presented two methods to represent the load-contours in L-shaped columns and to use them to determine the ultimate load.

Method (I) is based on the failure surfaces in a column and the actual shapes of load-contours are developed using an inverse method of analysis. Method (II) proposes to be replaced by the simple analysis of an equivalent square or rectangular column.

There are very few test results of L-shaped column to study its behavior since most experimental work in column research for biaxial bending and compression was limited primarily to rectangular, circular and octagonal cross sections.

A state of the art in the inelastic behavior of irregularly shaped columns is gaining momentum, as it is foreseeable that in future there will be an increased use of irregularly shaped columns. There is greater need of design aids and computer programs for column under biaxial bending and compression.

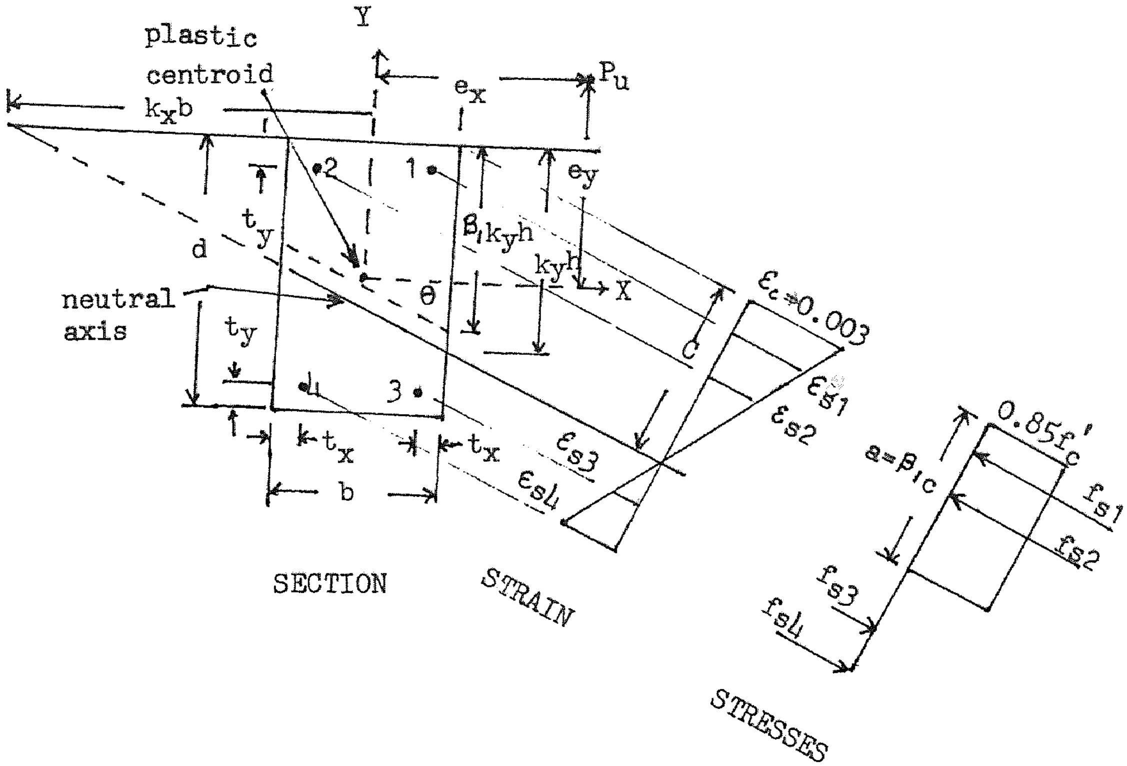

Fig. - 1.1 COLUMN SECTION WITH BIAXIAL BENDING AT THE ULTIMATE LOAD

CHAPTER II

TEST PROGRAM

A. DESCRIPTION OF TEST SPECIMENS

All together four specimens were tested. All columns were designed as short columns and were each six feet long. Physical characteristics of columns tested are shown in Table 5.1 and Fig. 2.1-2.2.

The brackets were heavily reinforced to prevent local failure. Three columns were reinforced longitudinally by 14 Grade 60 # 3 bars and one by Grade 40 # 3 bars as seen in Fig.2.1 These longitudinal bars were held together by 1/8 in. ties at spacing of 3 inches center to center. The stirrups and longitudinal bars were tied together using 16 gauge binding wire. The reinforcement was assembled into a unit before it was placed in the mold.

B. MATERIALS AND FABRICATION:

1. Cement. High early strength type III Portland Cement was used for all concrete mixes.

2. Sand. Crushed quartz sand was used as

aggregates.

3. Concrete Mix. The concrete mix was of following proportions, specified by weight:

The water-cement ratio varied from 0.65 to 0.7.

The cement-sand ratio varied from 3 to 3.2.

Sand was used as aggregates. Coarse aggregates were not used.

4. Steel Reinforcement. Grade 40 and Grade 60 #3 bars (Diameter= 0.375 in., Area=0.11 in .) were used in all columns for main reinforcing steel. Grade 40 #1 (Diameter=0.125 in., Area=0.1226 in.) were used for stirrups. The main reinforcement and stirrups were carefully bent to the required shapes. Gauge 16 binding wire was used to hold the main reinforcement and stirrups together.

C. FORMWORK, CASTING AND CURING

1. Formwork. The form was built using 5/8 in. thick plywood. The formwork was built in sections which were connected together by screws to ensure ease of removal of the cast specimens and to allow repeated use of the form. The plywood was braced horizoantally and vertically using 2 x 4 in. wooden pieces to prevent buldging of the side walls. The form was

cleaned and oiled with a thin layer of motor oil to facilitate the easy removal of specimens.

2. Casting and curing. The test specimens were cast in horizontal position. This kind of casting is more practical as compared to the vertical casting. While a horizontal casting causes a strength differential across the column section, vertical casting will cause a differential in concrete quality along the column length After the concrete was placed in the form, it was compacted by means of a high frequency vibrator. Standard 3x6 and 6x12 in. cylinders were cast.

The test specimens and the cylinders were cured in the molds two days before removing the molds. The test specimens and cylinders were then cured for six days.

D. INSTRUMENTATION

1. Strain and Curvature Measurements :

The measurements of strain and curveture were done by the Demec Gauge Method. Six inches-range dial gauge with a least count of 0.0001 in. was used to measure the strain between a pair of demec gauges.

2. Deflection Measurements :

Ames dial gauges (range=2 in., least count=0.001 in.) were used to measure the mid-span deflections.

3. Loading Method :

The columns were tested in the horizontal position. The coloumns were loaded using the Enerpac 100 ton capacity hydraulic cylinder ram (effective area = 20.63 in .). Manual Enerpac pump model PEM 2042 with a maximum pressure of 10000 psi was used to drive the ram.

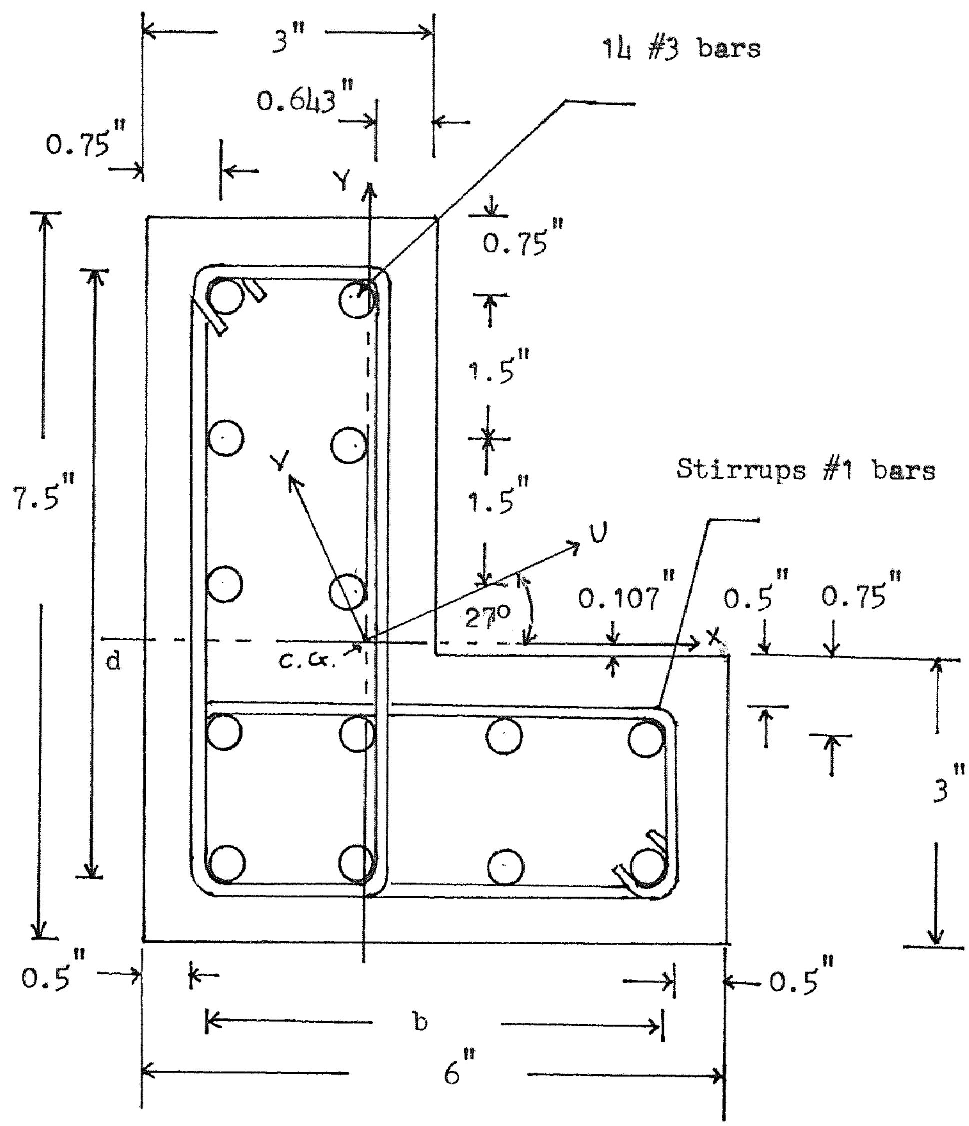

Fig. - 2.1 CROSS SECTION OF COLUMNS

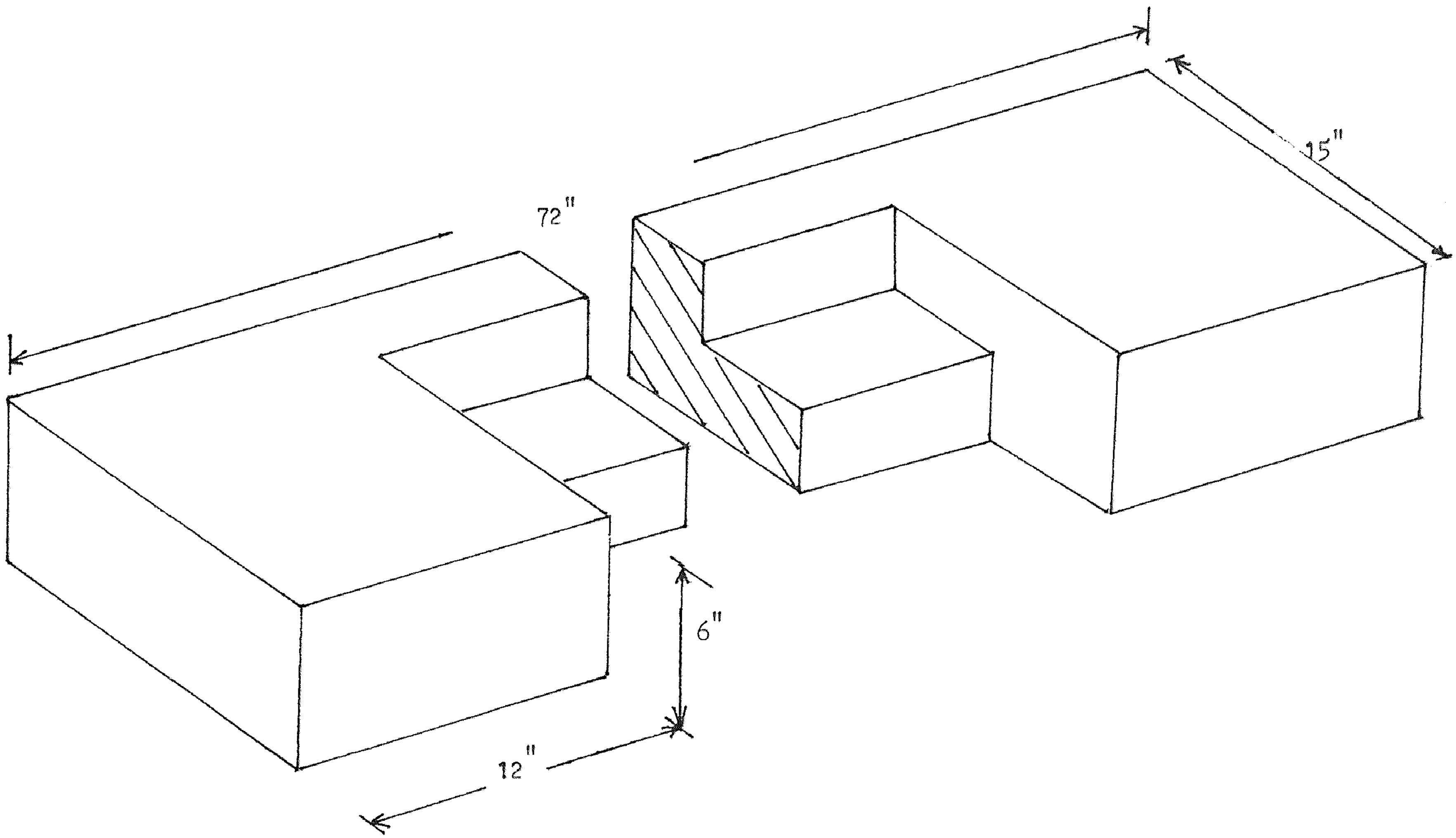

Fig. - 2.2 TEST SPECIMEN DETAILS

CHAPTER III

TEST PROCEDURE

A. COLUMN TESTS

The points of application of load were marked on the faces of brackets. The specimens were placed in the area of the loading frame using a 1 ton crane and were supported on roller supports built up to the required height by the use of pieces of styrofoam and wooden blocks.

All the columns were carefully centered in the testing machine and steel plates were put against the faces of each bracket to transfer the load to the column. All the columns were pin ended. A small initial load was applied to hold the column and steel plates in place.

The Ames dial gauges were then placed. The demec gauges were glued to the specimen earlier. The initial readings were taken for all the instruments. The minimum and maximum increments in load were 100 psi and 300 psi respectively. The roller supports were taken out when the applied load reached a value of 1000 psi.

After each increment of load, the machine was operated so as to hold the load constant, until the deflections come to rest at a reading. Then all gauges were read. This continued until the failure of the specimen. The complete test duration excluding the time required for the experimental setup was about 1.5 hours.

In general all specimens were tested using "controlled load " rather than "controlled deformation ". Stress and strain values for column #4 at each stage of loading are given in Table 5.3 .

Standard 3 x 6 and 6 x 12 in. cylinders were cast for each batch of concrete. The cylinders were capped using a sulpher compound the day before the test. Then following the test the cylinders were tested. A soil Test 400,000 pound capacity hydraulic testing machine was used. Standard cylinder strengths ranged from 3900 to 4200 psi. The values of f'_c for each column are given in Table 5.1 .

B. REINFORCEMENT TESTS :

Random samples of the bars were taken from all batches and tested in a Universal Testing machine.

Twenty three in. test specimens were cut from the #3 bars and marked at two points equidistant from the center and 6 in. apart. Strain measurements were taken by using demec gauge with a least count of 0.0001 in. The tests were "load-controlled". The resulting stress-strain curves for the main steel are shown in Fig. 3.1-3.2.

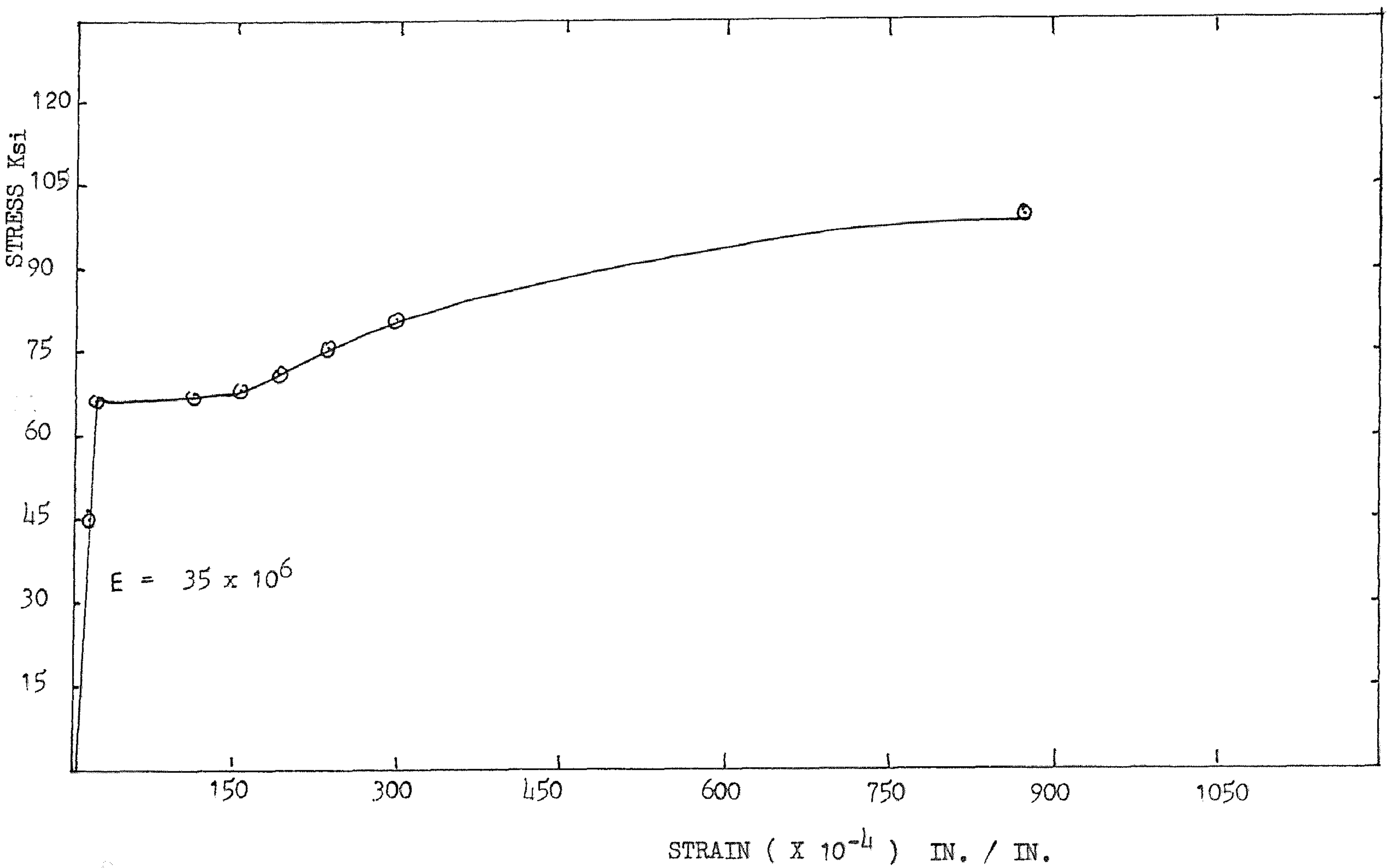

Fig. - 3.1 STRESS-STRAIN CURVE FOR REINFORCEMENT (N3S #3 BARS)

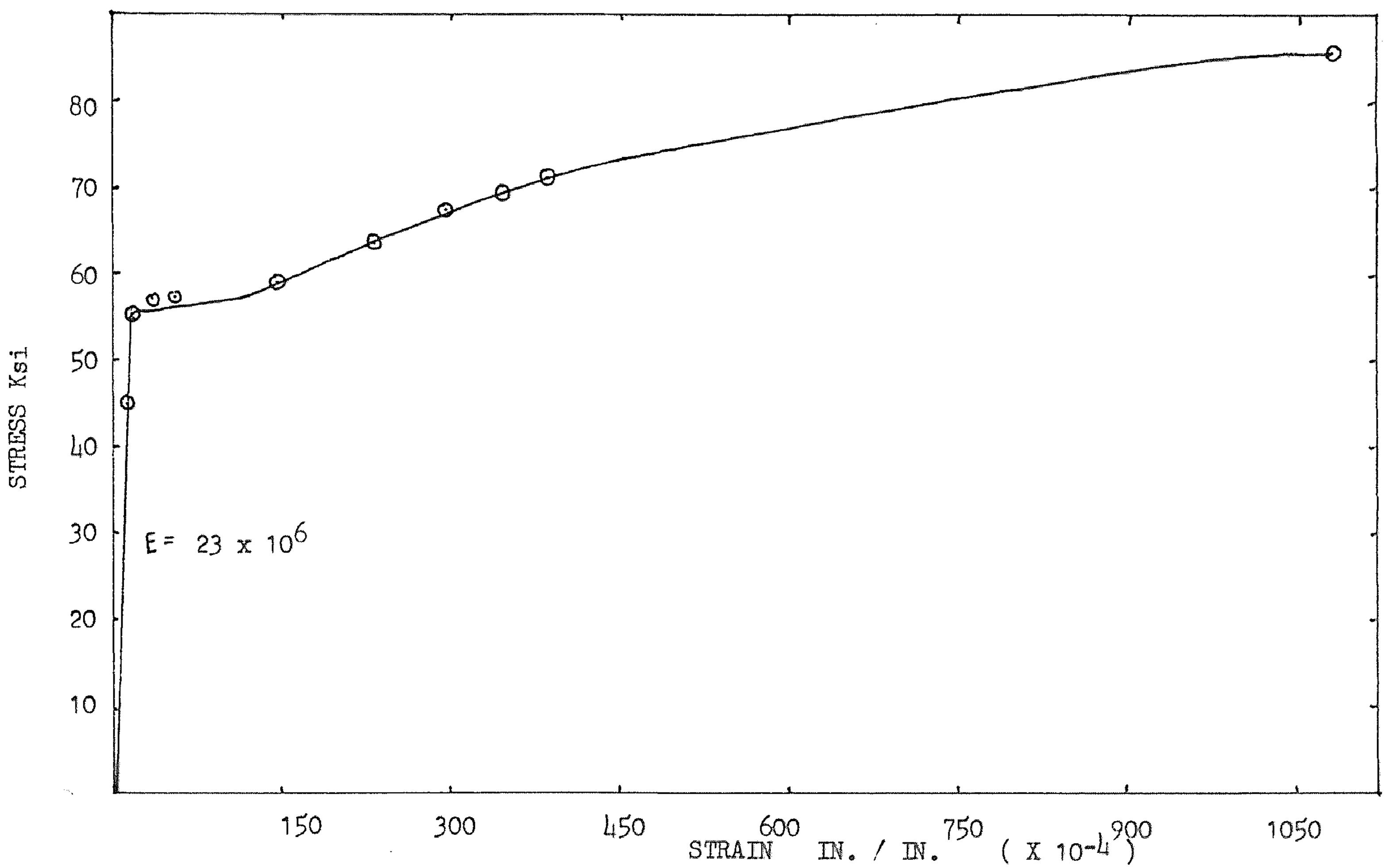

Fig. 3.2 - STRESS-STRAIN CURVE FOR REINFORCEMENT (BV3S #3 BARS)

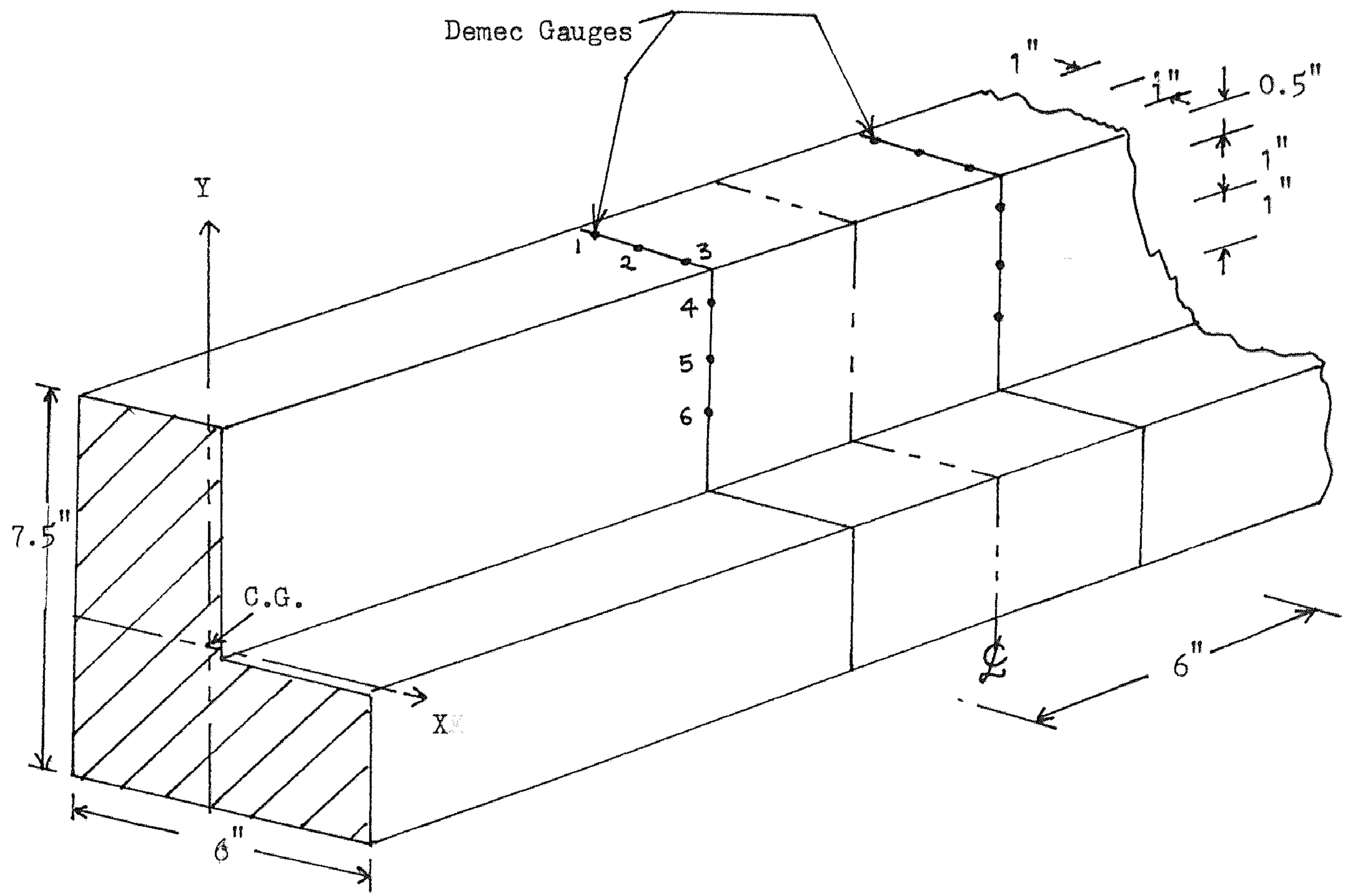

Fig. - 3.3 ARRANGEMENT OF DEMEC GAUGES

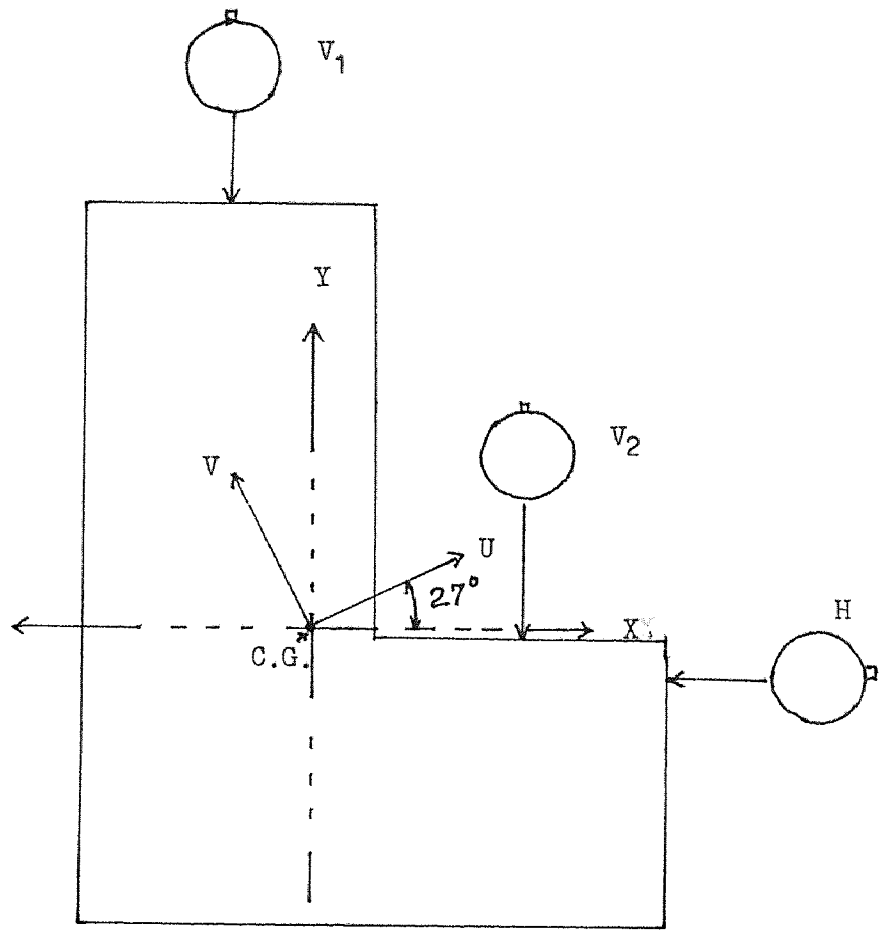

Fig. 3.4 ARRANGEMENT OF DEFLECTION GAUGES

Fig. - 3.5 FAILURE ZONE OF COLUMN #2

Fig. - 3.6 FAILURE ZONE OF COLUMN #3

Fig. - 3.7 FAILURE ZONE OF COLUMN #4

Fig. - 3.8 TEST SPECIMENS

CHAPTER IV

THEORETICAL ANALYSIS AND COMPUTER PROGRAM

A. INTRODUCTION AND ASSUMPTIONS

Theoretical analysis of the moment-curvature and load-deformation characteristics was carried out using the computer program developed by Hsu(1). This computer program gives the information for the stress and strain distribution across the section, the ultimate load and interaction surface of biaxially loaded short columns. It can also calculate the load-deformation curves from zero to maximum moment capacity using a "load control" process in the case of biaxial bending and axial compression.

The following assumptions have been made in this theoretical analysis.

1. The bending moments are applied about the principal axes of the section.

2. Plane sections remain plane before and after bending.

3. The longitudinal stress at a point is a function of the longitudinal strain at that point. The effect

of creep and shrinkage are ignored.

4. The stress-strain curves for the materials used are known

5. Stress reversal does not occur.

6. The effect of deformation due to shear and torsion and impact effects are negligible.

7. The section does not buckle before the ultimate load is attained.

8. Perfect bond exists between the concrete and reinfocing steel.

B. THEORETICAL DEVELOPMENT

The cross section of the structural member is divided into several small elements. Consider an element k with its centroid at point (X ,Y) referred to the axes of the symmetry (Fig. 4.2). The strain across the element k can be assumed to be uniform, since plane sections remain plane during bending,

$$\varepsilon_k = \varepsilon_p + \phi_x Y_k + \phi_y X_k \qquad \text{..............(4.1)}$$

Where ,

ε_p = Uniform direct strain due to an axial load P (Fig. 4.2)

ϕ_x = The curvature produced by the bending moment component M_x and is considered positive when it causes compressive strain in the positive Y-direction.

ϕ_y =The curvature produced by the bending moment component M_y and is considered positive when it causes compression in the positive X-direction.

Hsu(1) has modified Cranston(19) and Chatterji's stress-strain curves for the concrete as shown in Fig. 4.3a These curves account for the strain softening of concrete and the confined concrete elements maintained. The experimental stress-strain curve for steel has been idealized using piece-wise linear approximation to the curve in the strain-hardening region as shown in Fig. 4.3b .

Once the strain distribution across the section is established, the axial force P and moment components M_x and M_y can be calculated using the following equations :

$$P_{(c)} = \sum_{k=1}^{n} f_k \, a_k \qquad \text{..................(4.2)}$$

$$M_{x(c)} = \sum_{k=1}^{n} f_k \, a_k \, Y_k \qquad \text{..................(4.3)}$$

$$M_{y(c)} = \sum_{k=1}^{n} f_k \, a_k \, X_k \qquad \text{..................(4.4)}$$

Subscript (c) indicates values of P, M_x and M_y calculated in an iteration cycle and a_K is the area of element K. For a given section (known geometry and material properties) the stress resultants P, M_x and M_y can be expressed as functions of ϕ_x, ϕ_y and ε_p and given by the following equations :

$$P = P(\phi_x, \phi_y, \varepsilon_p) \qquad \text{................(4.5)}$$

$$M_x = M_x(\phi_x, \phi_y, \varepsilon_p) \qquad \text{................(4.6)}$$

$$M_y = M_y(\phi_x, \phi_y, \varepsilon_p) \qquad \text{................(4.7)}$$

$$M_{x(s)} = P_{(s)}\, e_y \qquad \text{................(4.8)}$$

$$M_{y(s)} = P_{(s)}\, e_x \qquad \text{................(4.9)}$$

P(s), M_X(s) and M_Y(s) can be expressed in terms of P(c), M_X(c) and M_Y(c). Using Taylor's expansion retaining linear terms as follows:

$$P_{(s)} = P_{(c)} + \frac{\partial P(c)}{\partial \phi_x}\,\delta\phi_x + \frac{\partial P(c)}{\partial \phi_y}\,\delta\phi_y + \frac{\partial P(c)}{\partial \varepsilon_p}\,\delta\varepsilon_p \qquad \text{....(4.10)}$$

$$M_{x(s)} = M_{x(c)} + \frac{\partial M_{x(c)}}{\partial \phi_x} \delta\phi_x + \frac{\partial M_{x(c)}}{\partial \phi_y} \delta\phi_y + \frac{\partial M_{x(c)}}{\partial \varepsilon_p} \delta\varepsilon_p \quad \ldots .(4.11)$$

$$M_{y(s)} = M_{y(c)} + \frac{\partial M_{y(c)}}{\partial \phi_x} \delta\phi_x + \frac{\partial M_{y(c)}}{\partial \phi_y} \delta\phi_y + \frac{\partial M_{y(c)}}{\partial \varepsilon_p} \delta\varepsilon_p \quad ..(4.12)$$

Let

$$u' = P_{(c)} - P_{(s)} \quad \ldots\ldots\ldots\ldots\ldots(4.13)$$

$$v' = M_{x(c)} - M_{x(s)} \quad \ldots\ldots\ldots\ldots\ldots(4.14)$$

$$w' = M_{y(c)} - M_{y(s)} \quad \ldots\ldots\ldots\ldots\ldots(4.15)$$

Then equations (4.10-4.12) can be written as:

$$- u' = \frac{\partial P(c)}{\partial \varepsilon_p} \delta\varepsilon_p + \frac{\partial P(c)}{\partial \phi_x} \delta\phi_x + \frac{\partial P(c)}{\partial \phi_y} \delta\phi_y \quad \text{...........(4.16)}$$

$$- v' = \frac{\partial M_x(c)}{\partial \varepsilon_p} \delta\varepsilon_p + \frac{\partial M_x(c)}{\partial \phi_x} \delta\phi_x + \frac{\partial M_x(c)}{\partial \phi_y} \delta\phi_y \quad \text{.......(4.17)}$$

$$- w' = \frac{\partial M_y(c)}{\partial \varepsilon_p} \delta\varepsilon_p + \frac{\partial M_y(c)}{\partial \phi_x} \delta\phi_x + \frac{\partial M_y(c)}{\partial \phi_y} \delta\phi_y \quad \text{.......(4.18)}$$

An increment in axial force $\delta P(c)$ produces an increment of strain, $\delta\varepsilon_p$, at each element in the section. The corresponding stress change at element k is therefore $\delta\varepsilon_p(E_t)_k$. The resulting change $\delta P(c)$ in P(c) is given by :

$$\delta P_{(c)} = \sum_{k=1}^{n} (E_t)_k \, a_k \, \delta\varepsilon_p \quad \text{..........(4.19)}$$

Therefore,

$$\frac{\partial P(c)}{\partial \varepsilon_p} = \sum_{k=1}^{n} (E_t)_k \, a_k \quad \text{...........(4.20)}$$

Similarly, the changes $M_x(c)$ and $M_y(c)$ can be expressed in terms of $\delta\varepsilon_p$ and lead to the equations:

$$\frac{\partial M_x(c)}{\partial \varepsilon_p} = \sum_{k=1}^{n} (E_t)_k\, a_k\, Y_k \qquad \text{.............(4.21)}$$

$$\frac{\partial M_y(c)}{\partial \varepsilon_p} = \sum_{k=1}^{n} (E_t)_k\, a_k\, X_k \qquad \text{.............(4.22)}$$

similar expressions can be derived for $\delta P(c)$, $\delta M_x(c)$ and $\delta M_y(c)$ in terms of changes $\delta\phi_x$ and $\delta\phi_y$ and yield the following results:

$$\frac{\partial P(c)}{\partial \phi_x} = \sum_{k=1}^{n} (E_t)_k\, a_k\, Y_k \qquad \text{.............(4.23)}$$

$$\frac{\partial M_x(c)}{\partial \phi_x} = \sum_{k=1}^{n} (E_t)_k\, a_k\, Y_k^2 \qquad \text{.............(4.24)}$$

$$\frac{\partial M_y(c)}{\partial \phi_x} = \sum_{k=1}^{n} (E_t)_k\, a_k\, X_k\, Y_k \qquad \text{.............(4.25)}$$

$$\frac{\partial P(c)}{\partial \phi_y} = \sum_{k=1}^{n} (E_t)_k\, a_k\, X_k \qquad \text{.............(4.26)}$$

$$\frac{\partial M_x(c)}{\partial \phi_y} = \sum_{k=1}^{n} (E_t)_k\, a_k\, X_k\, Y_k \qquad \text{.............(4.27)}$$

$$\frac{\partial M_y(c)}{\partial \phi_y} = \sum_{k=1}^{n} (E_t)_k\, a_k\, X_k^2 \qquad \text{.............(4.28)}$$

Equations (4.19-4.28) and (4.16-4.18) can be arranged in a matrix form as shown in equations (4.29-4.31) to give the rates of change of P, M_x, and M_y due to changes in ε_p, ϕ_x and ϕ_y ;

$$\begin{bmatrix} \sum_{k=1}^{n} (E_t)_k a_k & \sum_{k=1}^{n} (E_t)_k a_k Y_k & \sum_{k=1}^{n} (E_t)_k a_k X_k \\ & \sum_{k=1}^{n} (E_t)_k a_k Y_k^2 & \sum_{k=1}^{n} (E_t)_k a_k X_k Y_k \\ \text{Symmetric} & & \sum_{k=1}^{n} (E_t)_k a_k X_k^2 \end{bmatrix} \begin{bmatrix} \delta\varepsilon_p \\ \delta\phi_x \\ \delta\phi_y \end{bmatrix} = - \begin{bmatrix} u' \\ v' \\ w' \end{bmatrix} \qquad \text{......(4.29)}$$

or

$$[K] \begin{bmatrix} \delta\varepsilon_p \\ \delta\phi_x \\ \delta\phi_y \end{bmatrix} = - \begin{bmatrix} u' \\ v' \\ w' \end{bmatrix} \qquad \text{........(4.30)}$$

or

$$\begin{bmatrix} \delta\varepsilon_p \\ \delta\phi_x \\ \delta\phi_y \end{bmatrix} = - [K]^{-1} \begin{bmatrix} u' \\ v' \\ w' \end{bmatrix} \qquad \text{.........(4.31)}$$

The values of u', v', w' can be selected to suit the accuracy required and their substitution in equation (4.31) at the end of m^{th} iteration cycle yields the values of $\delta\varepsilon_p$, ϕ_x and ϕ_y which lead to values of ε_p, ϕ_x and ϕ_y for the $(m+1)^{th}$ iteration cycle as follows:

$$\varepsilon_{p(m+1)} = \varepsilon_{p(m)} + \delta\varepsilon_p \qquad \text{.............(4.32)}$$

$$\phi_{x(m+1)} = \phi_{x(m)} + \delta\phi_x \qquad \text{.............(4.33)}$$

$$\phi_{y(m+1)} = \phi_{y(m)} + \delta\phi_y \qquad \text{.............(4.34)}$$

Once convergence is obtained within specified tolerances the computer program takes up the next load level and repeats the entire procedure.

For further detailed information about theory refer to(1).

C. THE COMPUTER PROGRAM

The computer program has to have the initial loads and curvature to start it. This is within the main program. Then the load, M_x, M_y, and ϕ_x , ϕ_y are calculated. Then the load is incremented by an amount that can be adjusted within the main program. Again the M_x, ϕ_x, M_y and ϕ_y are calculated. This occurs until either subroutine which calculates inverses fails or divergence occurs. In this fashion the complete behavior of the column can be obtained.

2. Analytical Investigations. Hsu and Mirza(21) proposed the approximate equations using the well-known modified moment-area theorem to evaluate the central deflection and rotations. The equations are as follows :

$$\delta_{2x} = \frac{\phi_y l^2}{8} \qquad \text{..........(4.35)}$$

$$\delta_{2y} = \frac{\phi_x l^2}{8} \qquad \text{..........(4.36)}$$

The axial load is incremented by P with the factors which related to the effect of the mid-span deflection. The equations are as follows :

(a) in case of loading condition as shown in Fig. 4.4 .

$$P_3 = \frac{P_1 (e_x^2 + e_y^2)}{((e_x + \delta_{2y})^2 + (e_y + \delta_{2x})^2)} \qquad \text{.......(4.37)}$$

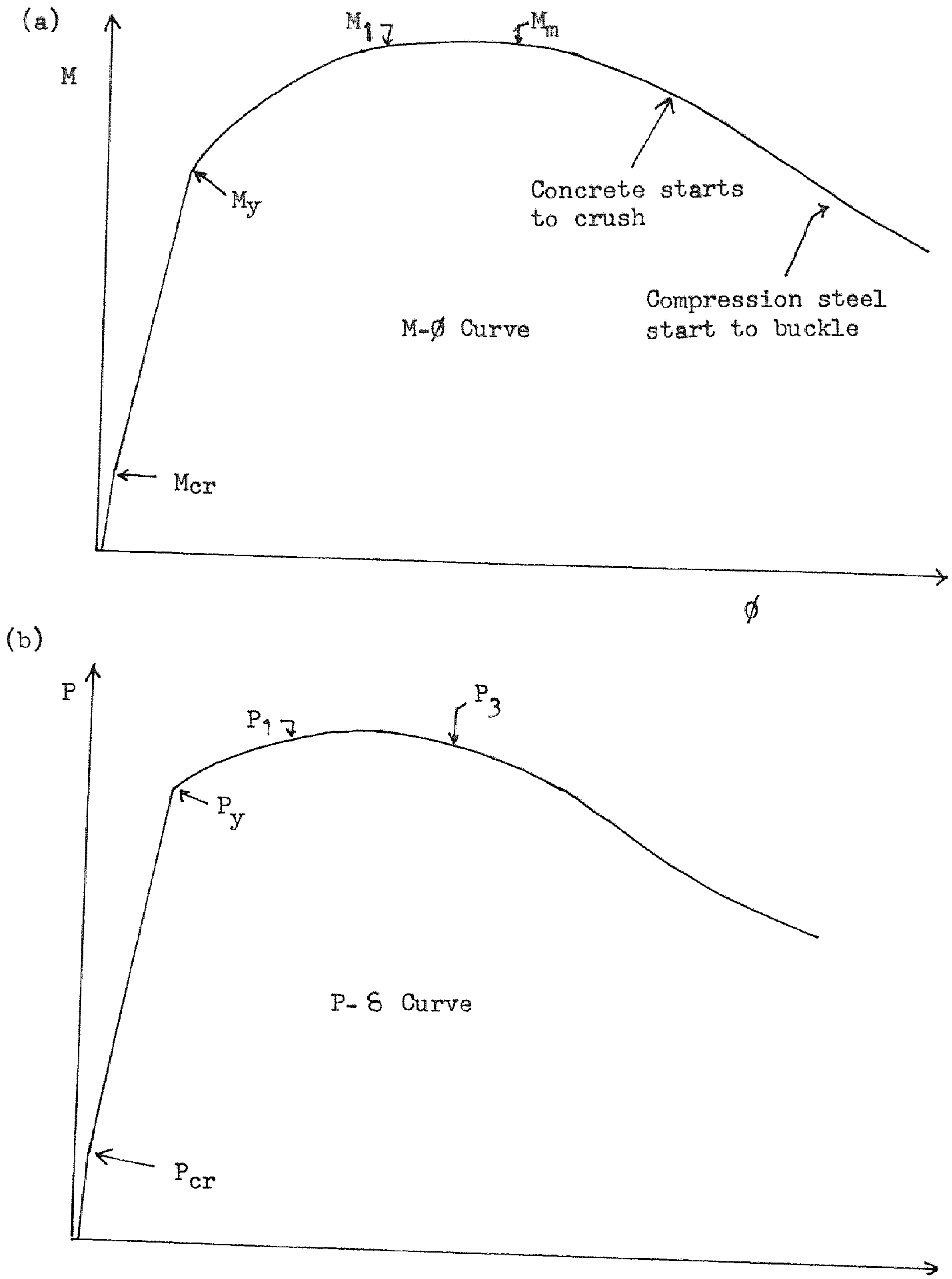

Fig. - 4.1 TYPICAL RELATIONSHIP BETWEEN M-Ø AND P-δ CURVES FOR SHORT COLUMN

(a)

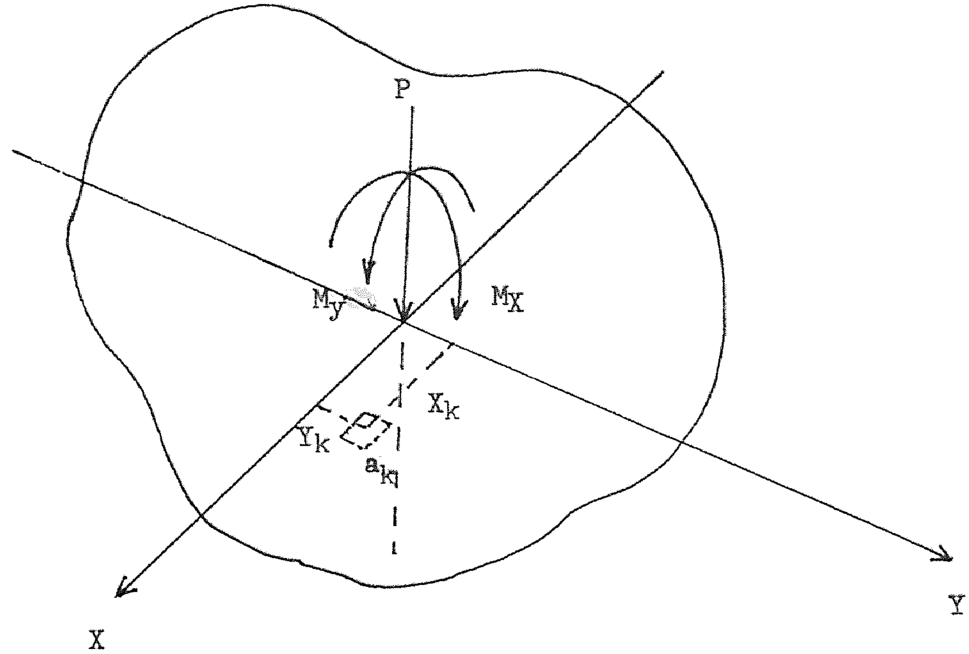

(b)

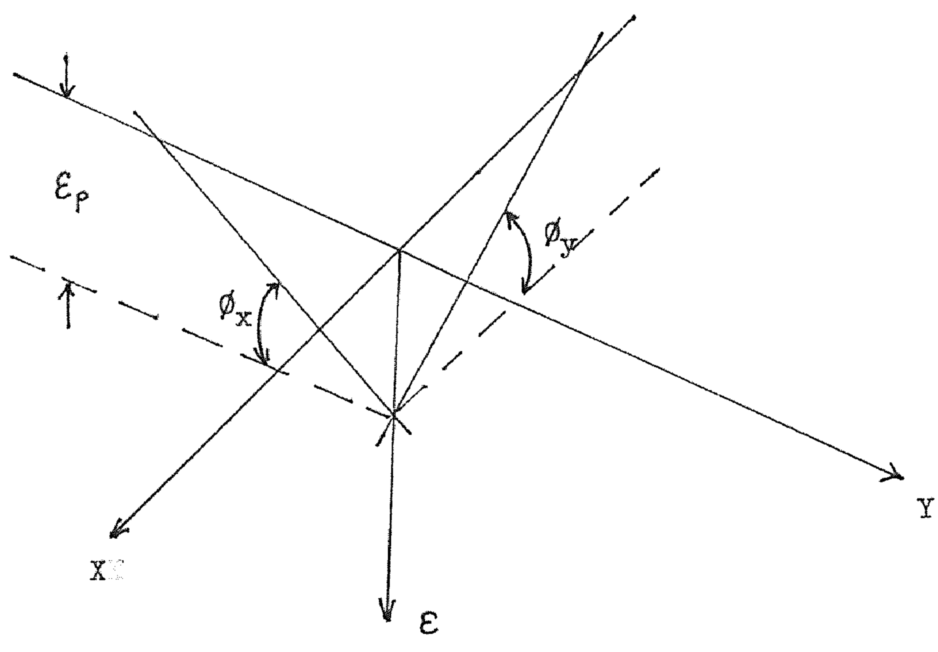

Fig. - 4.2 IDEALIZATION OF A CROSS-SECTION SUBJECTED TO BIAXIAL BENDING AND AXIAL LOAD

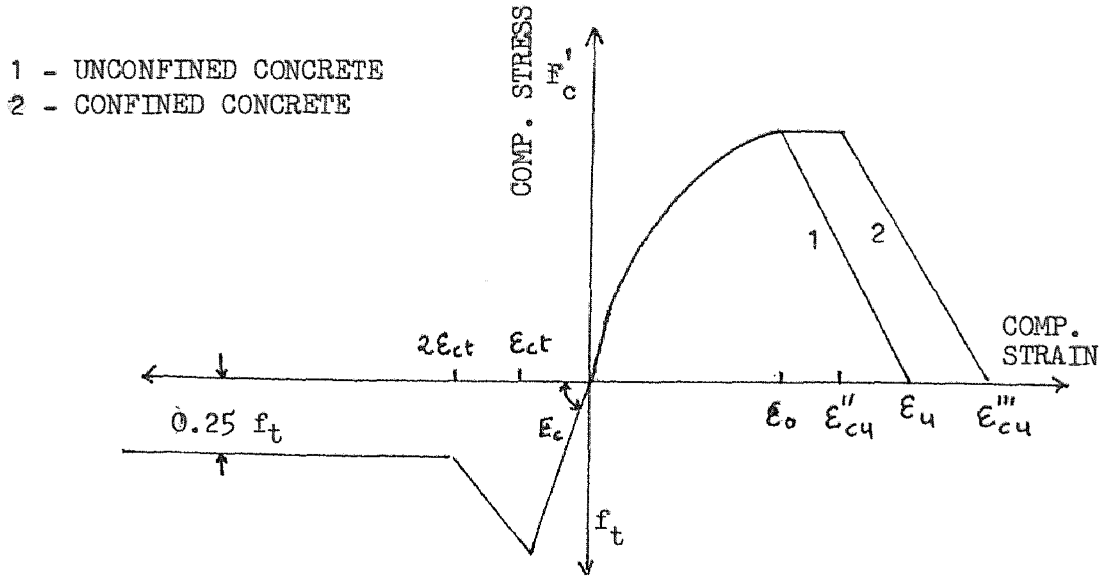

Fig. - 4.3a IDEALIZED STRESS-STRAIN CURVES FOR CONCRETE

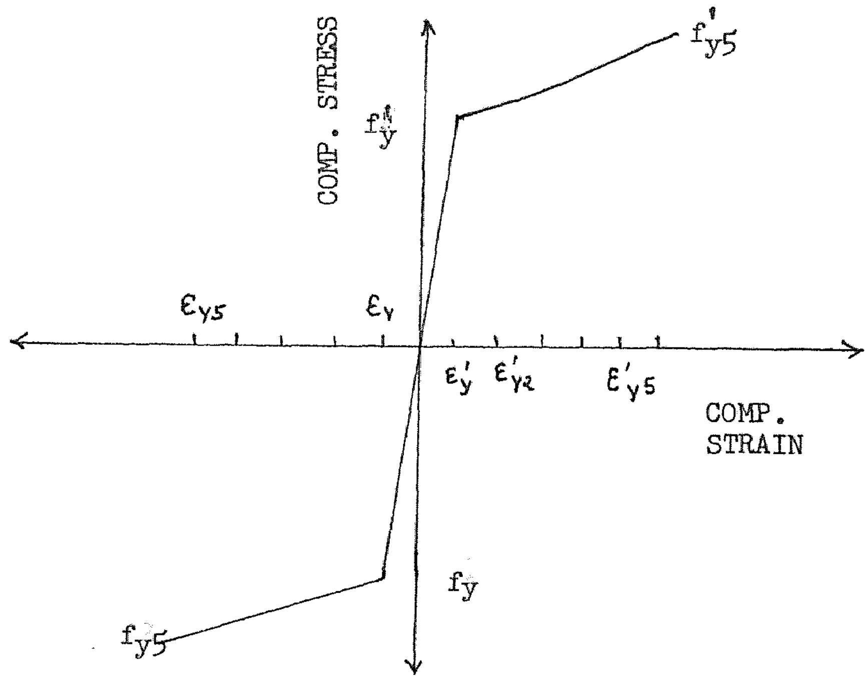

Fig. - 4.3b IDEALIZED STRESS-STRAIN CURVE FOR STEEL

(a)

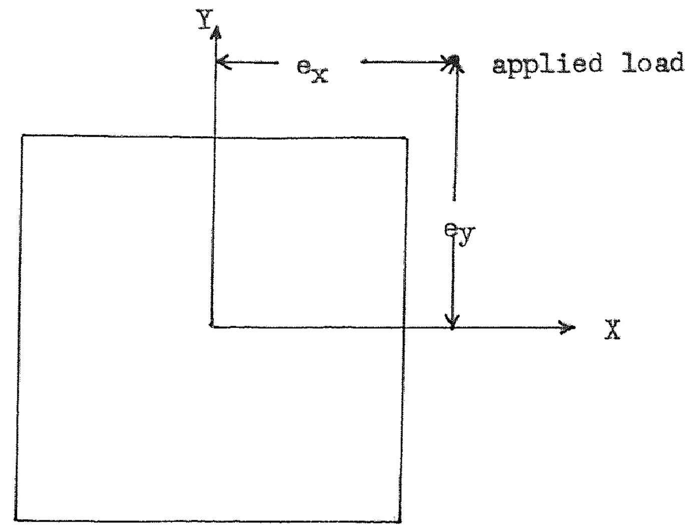

(b)

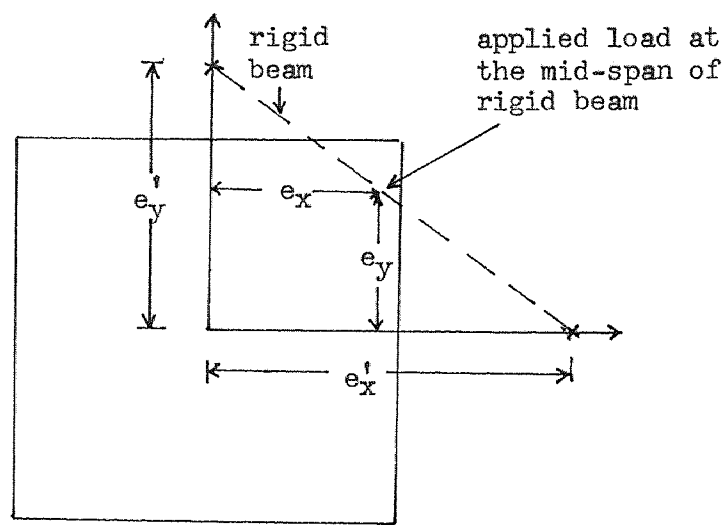

Fig. - 4.4 LOADING CONDITIONS FOR BIAXIALLY LOADED SHORT COLUMN

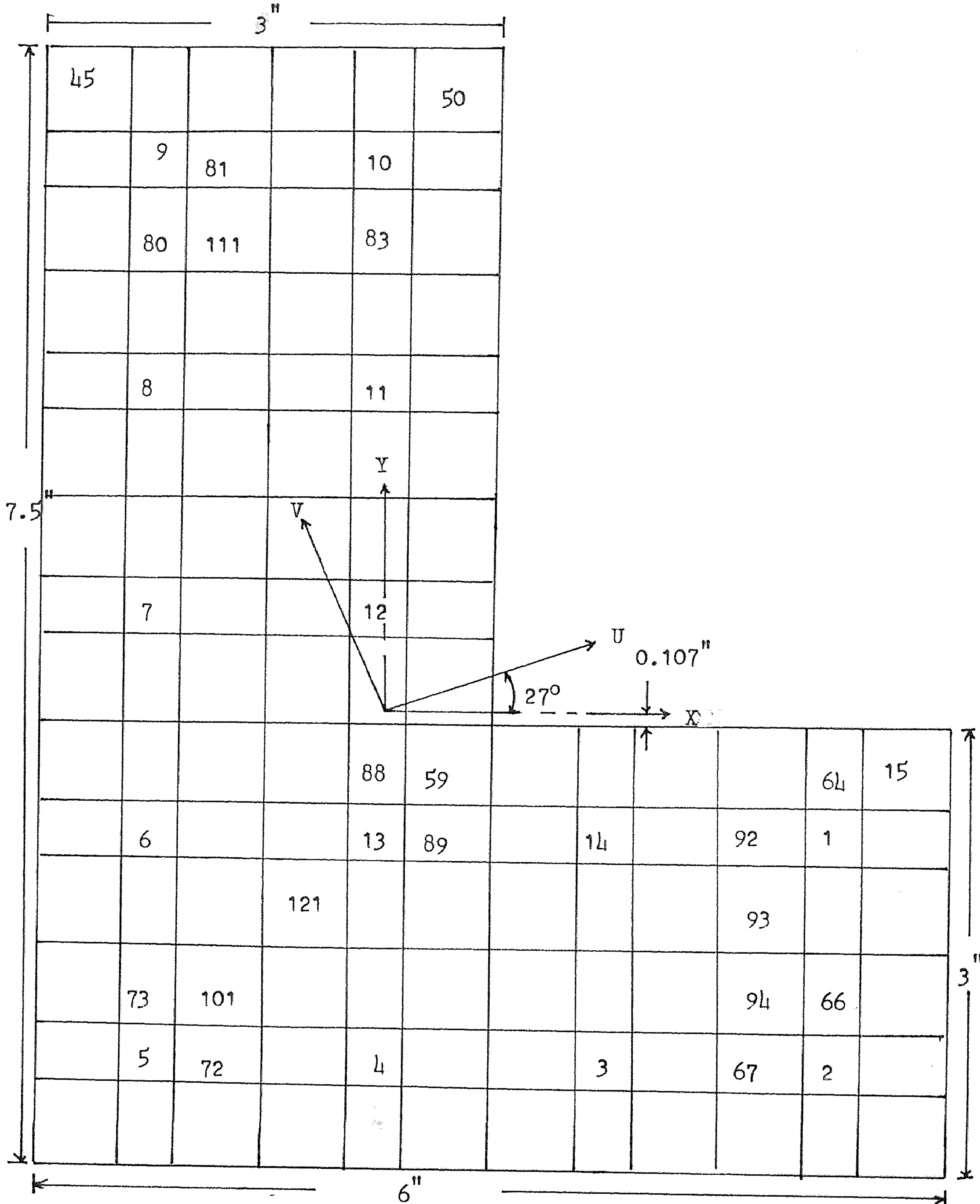

Fig. - 4.5 CROSS-SECTION SHOWING ALL ELEMENTS

CHAPTER V

COMPUTER AND TEST RESULTS

A. COMPUTER RESULTS

1. Computer program developed by Hsu(1) was used to find the stress, strain distribution across the section, the ultimate strength, moments about the principal axes and curvature in the principal axes. These values of moments and curvatures about the principal axes are transfered to the centroidal axes X and Y. The transfered values of computer results are given in Table 5.6-5.8.

2. Transformation Matrix :

Since the principal axes are taken for analytical purpose co-ordinates transformation is an important procedure. From the strength of materials, the following steps can be used for transformation of co-ordinates, moments, and curvatures :

1. Find moment of inertia I_x, I_y and product moment of inertia I_{xy}.

2. Use equation $\tan 2\theta = 2I_{xy} / (I_y - I_x)$ to determine the angle between the centroidal and the

principal axes.

3. Use equation

$$\begin{bmatrix} u \\ v \end{bmatrix} = [R]\begin{bmatrix} x \\ y \end{bmatrix} \qquad \text{..........(5.1)}$$

Where,

$$[R] = \begin{bmatrix} \text{Cos}\theta & \text{Sin}\theta \\ -\text{Sin}\theta & \text{Cos}\theta \end{bmatrix} \qquad \text{..........(5.2)}$$

Following these steps the data for the specimens used in this study can be determined as follows :

$I_X = 144.8$ in^4.

$I_Y = 81.5$ in^4.

$I_{XY} = -43.4$ in^4.

$\theta = 27^\circ$

From the above investigation, the load, moment and curvature with respect to the principal axes U and V can be found easily. For practical purpose these results should be transfered to the centroidal axes X and Y.

Now consider the centroidal axes X and Y as global co-ordinate axes and the principal axes U and V as structural co-ordinate axes as shown in Fig. 5.1. The angle of rotation is considered in anticlockwise direction. The transformation matrix R′ can be obtained as follows (see Ref. 15) :

1. For the case (a) shown in Fig. 5.1a. the transformation is given by :

$$\left[R'\right] = \begin{bmatrix} \mathrm{Cos}\theta & \mathrm{Sin}\theta \\ -\mathrm{Sin}\theta & \mathrm{Cos}\theta \end{bmatrix} \quad \ldots\ldots\ldots(5.3)$$

Moments and curvatures about the centroidal axes in terms of the moment and the curvature about the principal axes can be given as follows :

$$\begin{bmatrix} M_x \\ M_y \end{bmatrix} = \left[R'\right] \begin{bmatrix} M_u \\ M_v \end{bmatrix} \quad \ldots\ldots\ldots(5.4)$$

$$M_x = M_u\,\mathrm{Cos}\theta + M_v\,\mathrm{Sin}\theta \quad \ldots\ldots\ldots(5.5)$$

$$M_y = M_v\,\mathrm{Cos}\theta - M_u\,\mathrm{Sin}\theta \quad \ldots\ldots\ldots(5.6)$$

and

$$\begin{bmatrix} \phi_x & \phi_{xy} \\ \phi_{xy} & \phi_y \end{bmatrix} = \left[R'\right]^T \begin{bmatrix} \phi_u & \phi_{uv} \\ \phi_{uv} & \phi_v \end{bmatrix} \left[R'\right] \quad \ldots(5.7)$$

since U and V are the principal axes, in both the cases (a) and (b) $\phi_{uv} = 0$ then,

$$\begin{bmatrix} \phi_x & \phi_{xy} \\ \phi_{xy} & \phi_y \end{bmatrix} = \begin{bmatrix} \text{Cos}\theta & -\text{Sin}\theta \\ \text{Sin}\theta & \text{Cos}\theta \end{bmatrix} \begin{bmatrix} \phi_u & 0 \\ 0 & \phi_v \end{bmatrix} \begin{bmatrix} \text{Cos}\theta & \text{Cos}\theta \\ -\text{Sin}\theta & \text{Cos}\theta \end{bmatrix} \quad ..(5.8)$$

$$= \begin{bmatrix} \text{Cos}\theta & -\text{Sin}\theta \\ \text{Sin}\theta & \text{Cos}\theta \end{bmatrix} \begin{bmatrix} \phi_u \ \text{Cos}\theta & \phi_u \ \text{Sin}\theta \\ -\phi_v \ \text{Sin}\theta & \phi_v \ \text{Cos}\theta \end{bmatrix} \quad ..(5.9)$$

$$= \begin{bmatrix} (\phi_u \ \text{Cos}^2\theta + \phi_v \ \text{Sin}^2\theta) & (\phi_u - \phi_v) \ \text{Sin}\theta \ \text{Cos}\theta \\ (\phi_u - \phi_v) \ \text{Sin}\theta \ \text{Cos}\theta & (\phi_u \text{Sin}^2\theta + \phi_v \text{Cos}^2\theta) \end{bmatrix} \quad ....(5.10)$$

Therefore,

$$\phi_x = \phi_u \ \text{Cos}^2\theta + \phi_v \ \text{Sin}^2\theta \quad ....(5.11)$$

$$\phi_y = \phi_u \ \text{Sin}^2\theta + \phi_v \ \text{Cos}^2\theta \quad ....(5.12)$$

2. For the case (b) shown in Fig. 5.1b, the transformation matrix is as follows :

Moments and curvatures about the centroidal axes can be expressed as follows :

$$R = \begin{bmatrix} \text{Cos}\theta & -\text{Sin}\theta \\ \text{Sin}\theta & \text{Cos}\theta \end{bmatrix} \qquad \text{............(5.13)}$$

$$\begin{bmatrix} M_x \\ M_y \end{bmatrix} = \begin{bmatrix} \text{Cos}\theta & -\text{Sin}\theta \\ \text{Sin}\theta & \text{Cos}\theta \end{bmatrix} \begin{bmatrix} M_u \\ M_v \end{bmatrix} \qquad \text{..........(5.14)}$$

$$M_x = M_u \text{ Cos}\theta - M_v \text{ Sin}\theta \qquad \text{..........(5.15)}$$

$$M_y = M_u \text{ Sin}\theta + M_v \text{ Cos}\theta \qquad \text{...........(5.16)}$$

and

$$\begin{bmatrix} \phi_x & \phi_{xy} \\ \phi_{xy} & \phi_y \end{bmatrix} = \left[R\right]^T \begin{bmatrix} \phi_u & 0 \\ 0 & \phi_v \end{bmatrix} \left[R\right] \qquad \text{..........(5.17)}$$

$$\phi_x = \phi_u \text{ Cos}^2\theta + \phi_v \text{ Sin}^2\theta \qquad \text{...........(5.18)}$$

$$\phi_y = \phi_u \text{ Sin}^2\theta + \phi_v \text{ Cos}^2\theta \qquad \text{............(5.19)}$$

In this study the equations for moments and curvatures those in case (a) are used.

Since, $\theta = 27^{\circ}$

$$M_x = 0.891\ M_u + 0.454\ M_v \qquad \text{.............}(\ 5.20\ )$$

$$M_y = 0.891\ M_v - 0.454\ M_u \qquad \text{.............}(\ 5.21\ )$$

$$\emptyset_x = 0.794\ \emptyset_u + 0.2061\ \emptyset_v \qquad \text{..............}(\ 5.22\ )$$

$$\emptyset_y = 0.794\ \emptyset_v + 0.2061\ \emptyset_u \qquad \text{..............}(\ 5.23\ )$$

B. TEST BEHAVIOR

The tests proceeded smoothly following the uncontrolled deformation loading procedure with the axial load maintained constant at each loading stage.

The development of cracks increased slowly as the load was increased. No signs of crushing or spalling of concrete were seen until ultimate load was reached. When the ultimate load was reached concrete spalling occured at the critical section. Typical failure zone of section is shown in Fig. 3.5-3.7. In most cases 1/2 to 1 in. thick concrete portion spalled off near the critical sections. Concrete spalling was followed by the post buckling of the compression steel. When the ultimate load was reached, large rotations and strains took place before the total collapse of the columns. Strains and rotations at the collapse could not be measured.

The average value of concrete strain over a 6 in. gauge length was 0.003936 in. / in. at the loading stage before the collapse. The maximum strain measured in the 6 in. gauge length was 0.004766 in. / in.

C. ANALYSIS OF TEST RESULTS

1. MOMENT CURVATURE RELATIONSHIP

The writer, in the present experimental investigation uses an approach in which the moments and curvatures are established along X and Y axes (X and Y axes pass through the centroid of the section). The moment-curvature relationships along X and Y axes are then compared with the results obtained using the computer program.

To obtain the strain distributions along X and Y axes demec gauge method was used. The typical demec-gauge arrangement for the measurement of strain values along X and Y axes are shown in Fig. 3.3. The demec gauge method is used as follows. The strain distribution across the XZ and YZ planes is found at each loading stage and is plotted against the distance between corresponding pair of demec gauges as shown in Fig. 5.2-5.7. When the strain distribution is nonlinear the curvature at particular loading stage is given by the following equation suggested by Mattock(25).

$$\phi = \frac{\varepsilon_{(c)}}{kd} \qquad \text{.............(5.24)}$$

ϕ = curvature

ε_c = Maximum compressive concrete strain and

kd = Distance from this maximum compressive concrete strain to the point of zero strain (or neutral axis)

Kd is obtained by drawing lines through the maximum concrete strain and the other strains until the neutral axis is bisected.

Moments, M_x and M_y are calculated as follows :

$$M_x = P\,(e_y + \delta_y) \qquad \text{.............(5.25)}$$

$$M_y = P\,(e_x + \delta_x) \qquad \text{.............(5.26)}$$

δ_y = Deflection in Y direction at mid-height of column

δ_x = deflection in X direction at mid-height of column

The curves of ε_c v/s distance between pairs of demec gauges for all columns are listed below.

Fig. 5.2-5.3 - column # 2

Fig. 5.4-5.5 - column # 3

Fig. 5.6-5.7 - column # 4

Tables listed below show experimental results for M_x, ϕ_x, M_y and ϕ_y. Here computer results for M_x, ϕ_x, M_y, and ϕ_y are also included.

Table 5.6 - column # 2

Table 5.7 - column # 3

Table 5.8 - column # 4

The curves of $M_x - \phi_x$ and $M_y - \phi_y$ plotted for all columns are listed below.

Fig. 5.8 - column #2 - M_x v/s ϕ_x

Fig. 5.9 - column # 2 - M_y v/s ϕ_y

Fig. 5.10 - column # 3 - M_x v/s ϕ_x

Fig. 5.11 - column # 3 - M_y v/s ϕ_y

Fig. 5.12 - column # 4 - M_x v/s ϕ_x

Fig. 5.13 - column # 4 - M_y v/s ϕ_y

A comparative study is discussed in chapter VI and in the conclusions.

2. LOAD - DEFLECTION RELATIONSHIPS

In fact it was not possible to measure the mid-height deflections. The deflections in X and Y direction were taken at sections few inches away from (6 in.) the mid-height.

Dial gauges with least count of 0.0005 and 0.001 in. were used. From the dial gauge readings at each loading stage deflections in X and Y directions are calculated. The tables listed below show the experimental results for load and deflection for column #4.

Table 5.4 - column # 4 P- δ_x

Table 5.5 - column # 4 P- δ_y

The figures listed below show the load-deflection curves.

Fig. 5.14 - column #2 P- δ_x

Fig. 5.15 - column #2 P- δ_y

Fig. 5.16 - column #3 $P-\delta_x$

Fig. 5.17 - column #3 $P-\delta_y$

Fig. 5.18 - column #4 $P-\delta_x$

Fig. 5.19 - column #4 $P-\delta_y$

Table : 5.1

SPECIMEN DETAILS

Col. #	Bars	f_y Ksi.	A in.^{2}	s in.	f_c' Psi.	e_x in.	e_y in.	l in.
2	14 #3	67.0	0.01227	3	4200	1.53	5.o	72
3	14 #3	67.0	0.01227	3	4200	1.68	5.5	72
4	14 #3	58.0	0.01227	3	4000	1.68	6.5	72

Table : 5.2

MEASURED VALUES OF CHANGES IN LENGTH BETWEEN PAIRS OF DEMEC GAUGES FOR COLUMN #4

Load	1	2	3	4	5	6
Psi.	All Readings X 10^{-6} (in.)					
150	2484	2400	0011	2248	2467	0023
334	2494	2415	0036	2297	2481	0037
600	0007	2433	0048	2329	2495	0049
800	0026	2459	0085	2373	0022	0085
1000	0044	2493	0134	2428	0062	0091
1250	0120	0108	0273	0034	0167	0160
1300	FAILURE					

Table : 5.3

STRAINS OF CONCRETE SURFACE BETWEEN PAIRS

OF DEMEC GAUGES FOR COLUMN #4

Load	1	2	3	4	5	6
Psi.	All Readings X 10^{-6} (in.)					
150	0.0	0.0	0.0	0.0	0.0	0.0
334	166.6	250.0	416.6	816.6	233.3	233.3
600	383.3	550.0	616.6	1350.0	466.6	433.3
800	700.0	983.3	1233.3	2083.3	916.6	1033.3
1000	1000.0	1550.0	2050.0	3000.0	1583.3	1133.3
1250	2266.0	3466.6	4366.6	4766.6	3333.3	2283.3

1300 FAILURE

Table : 5.4

LOAD V/S HORIZONTAL DEFLECTION CALCULATION FOR

COLUMN #4

Load (Psi.)	Load (Kips)	Horizontal Gauge (in.)	Horizontal Deflection (in.)
150	3.09	013	0.0
334	6.89	994	0.019
600	12.37	932	0.081
800	16.50	857	0.094
Reset		859	
1000	20.62	793	0.160
1250	25.78	540	0.413

1300 FAILURE

Table : 5.5

LOAD V/S VERTICAL DEFLECTION CALCULATION

FOR COLUMN #4

Load Psi.	Load (K)	Ver. Gau. #1 (in.)	Ver. Gau. #2 (in.)	Ver. Def. V_1 (in.)	Ver. Def. V_2 (in.)	Ver. Def. V (in.)
150	3.09	860	677	0.0	0.0	0.0
334	6.89	858	638	0.02	0.039	0.039
600	12.37	800	574	0.06	0.103	0.103
800	16.50	723	495	0.137	0.182	0.182
Reset		655	480			
1000	20.62	596	388	0.196	0.274	0.274
1250	25.78	350	142	0.442	0.520	0.520

1300 FAILURE

Table : 5.6

CALCULATIONS OF EXPERIMENTAL AND COMPUTER

M_x, ϕ_x , M_y, ϕ_y FOR COLUMN #2

Experiment					Computer				
Load Kip	Mx K-in	ϕ_x 1/in. X10^{-4}	M y K-in.	ϕ_y 1/in. X10^{-4}	Load K	M_x K-in.	ϕ_x 1/in. X10^{-4}	My K-in.	ϕ_y 1/in X10^{-4}
6.91	34.7	0.95	10.83	1.5	20.0	100.0	1.98	30.6	3.74
10.31	51.9	1.07	16.27	1.9	30.0	150.0	3.40	45.9	6.40
14.44	72.7	2.00	23.04	3.0	30.6	153.0	3.53	46.8	6.63
19.60	112.3	2.79	32.39	4.2	31.0	155.0	3.64	47.4	6.83
24.75	126.3	3.80	42.14	5.0	31.3	156.5	3.71	47.9	6.97
28.90	148.3	5.10	49.21	6.2	31.6	158.0	3.8	48.4	7.11
33.00	171.1	6.56	57.78	9.1					

38.16(Kips) FAILURE 37.85(Kips) FAILURE

e_x = 1.53 in.

e_y = 5 in.

Table : 5.7

CALCULATIONS OF EXPERIMENTAL AND COMPUTER

M_X, $\emptyset_X$, M_Y, $\emptyset_Y$ FOR COLUMN #3

Experiment					Computer				
Load Kip	M_X K-in	$\emptyset_X$ 1/in. $X10^{-4}$	M_Y K-in.	$\emptyset_Y$ 1/in. $X10^{-4}$	Load K	M_X K-in.	$\emptyset_X$ 1/in. $X10^{-4}$	M_Y K-in.	$\emptyset_Y$ 1/in. $X10^{-4}$
6.89	38.1	0.65	11.68	1.0	10.0	54.9	0.98	16.8	1.88
10.31	57.24	1.15	17.75	1.6	15.0	82.4	1.57	25.2	2.98
14.43	80.4	1.84	25.35	2.0	20.0	109.8	2.19	33.6	4.15
20.62	116.3	2.90	38.38	3.0	25.0	137.3	2.90	42.0	5.47
24.23	138.2	4.86	47.05	4.4	30.0	164.7	4.07	50.4	7.65
28.87	167.3	5.90	58.58	7.0	35.0	192.2	9.31	58.8	17.2
					35.02	192.3	9.43	58.9	17.4

35.062(Kips) FAILURE   35.02(Kips) FAILURE

e_X = 1.68 in.

e_Y = 5.5 in.

Table :5.8

CALCULATIONS OF EXPERIMENTAL AND COMPUTER

M_x, ϕ_x , M_y, ϕ_y FOR COLUMN #4

Experiment					Computer				
Load Kip	M_x K-in	ϕ_x 1/in. $X10^{-4}$	M_y K-in.	ϕ_y 1/in. $X10^{-4}$	Load K	M_x K-in.	ϕ_x 1/in. $X10^{-4}$	M_y K-in.	ϕ_y 1/in. $X10^{-4}$
6.89	44.9	1.40	11.70	1.0	10.0	65.0	1.62	16.8	3.03
12.37	81.2	2.39	21.87	1.7	15.0	97.5	2.64	25.3	4.89
16.50	110.5	4.0	29.27	3.4	20.0	124.0	3.91	33.2	7.18
20.62	138.1	7.80	37.95	5.4	25.0	162.5	7.08	42.0	12.9
25.78	178.9	11.25	54.00	11.7	25.3	164.4	7.54	42.5	13.8
					25.4	165.3	7.77	42.7	14.2

26.81(Kips) FAILURE 26.50(Kips) FAILURE

e_x = 1.68 in.

e_y = 6.5 in.

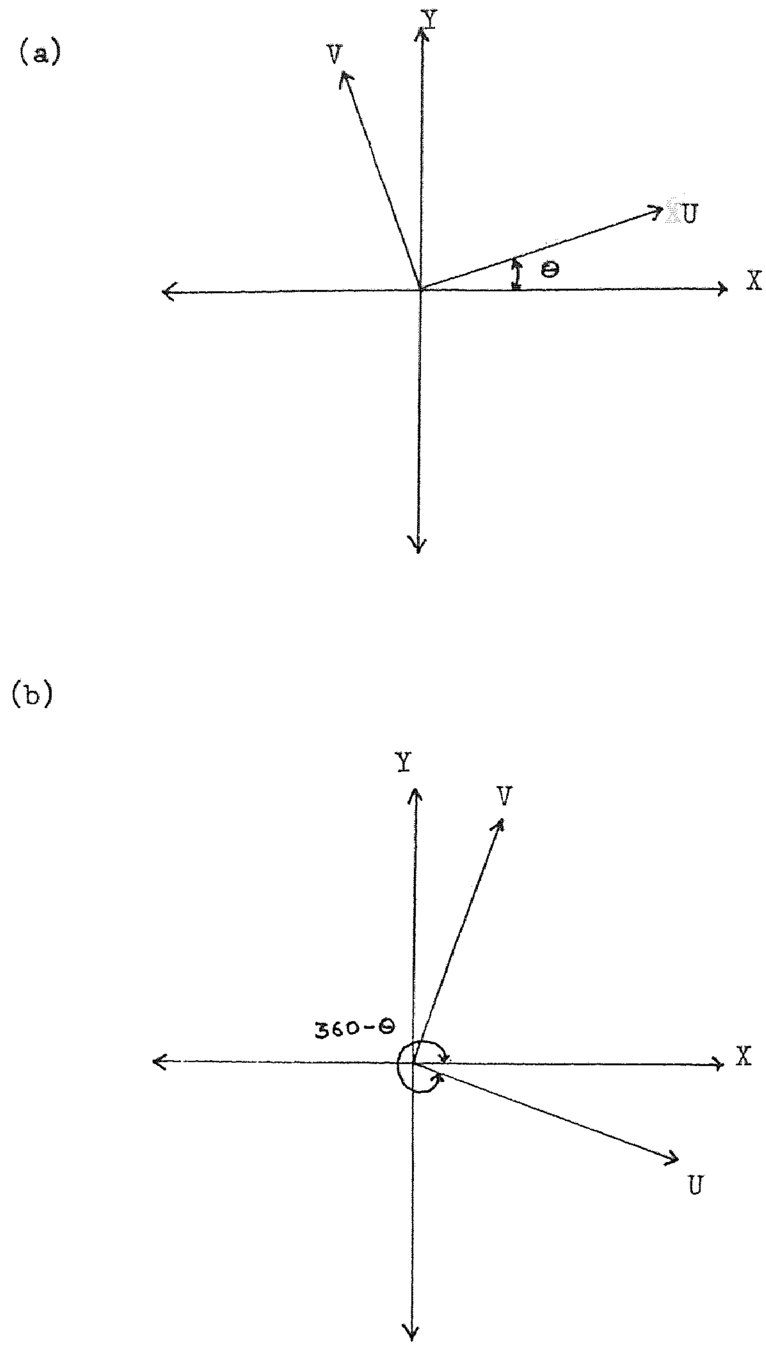

Fig. - 5.1 TRANSFORMATION OF AXES

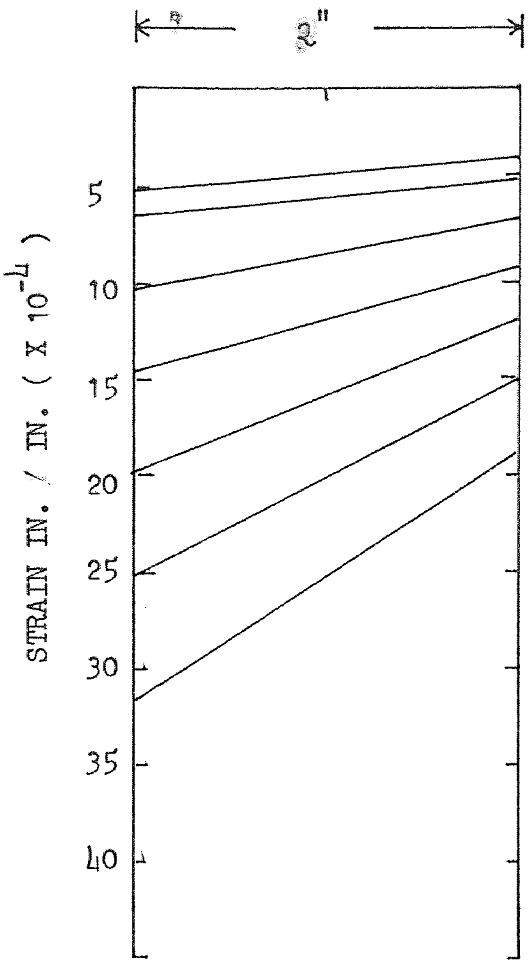

Fig. 5.2 STRAIN DISTRIBUTION LEADING TO ϕ_x
COLUMN #2

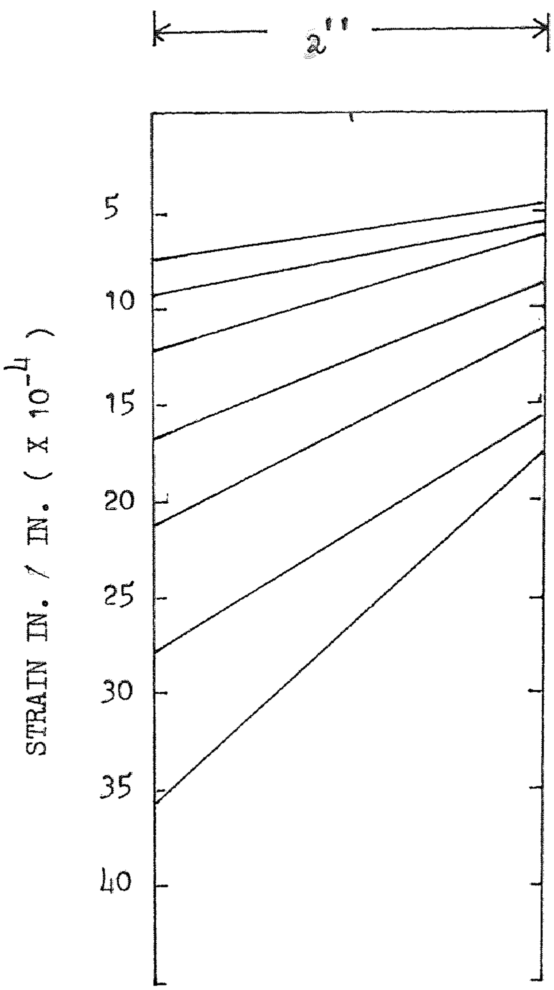

Fig. 5.3 STRAIN DISTRIBUTION LEADING TO ϕ_y
COLUMN #2

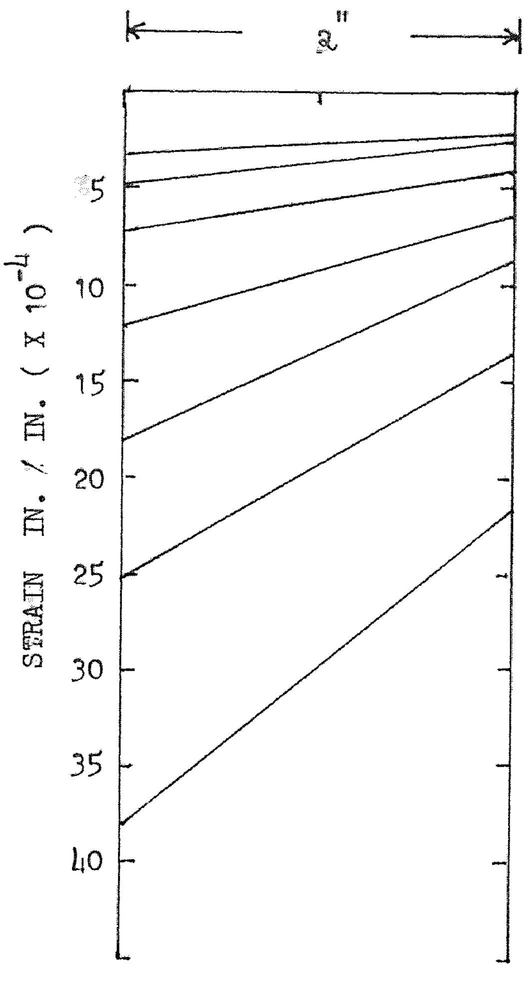

Fig. 5.4 STRAIN DISTRIBUTION LEADING TO ϕ_x
COLUMN #3

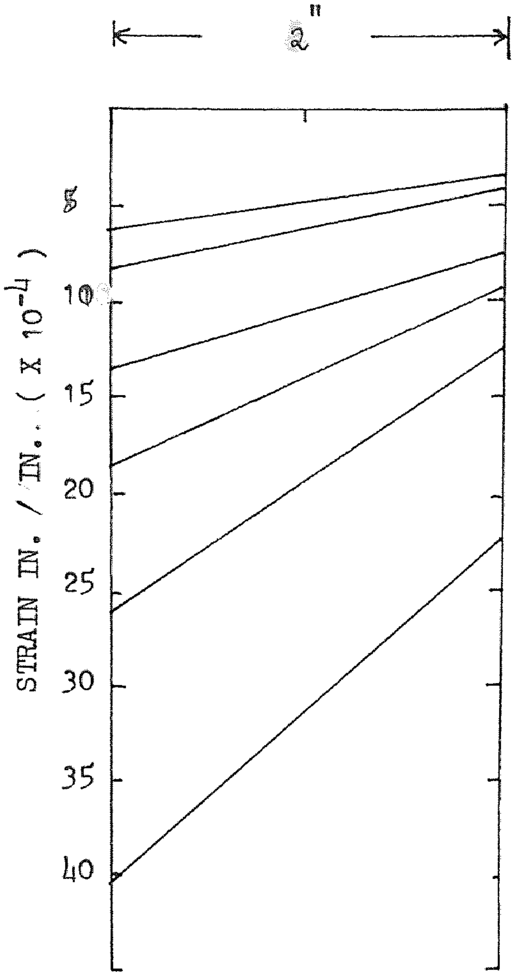

Fig. 5.5 STRAIN DISTRIBUTION LEADING TO ϕ_y
COLUMN #3

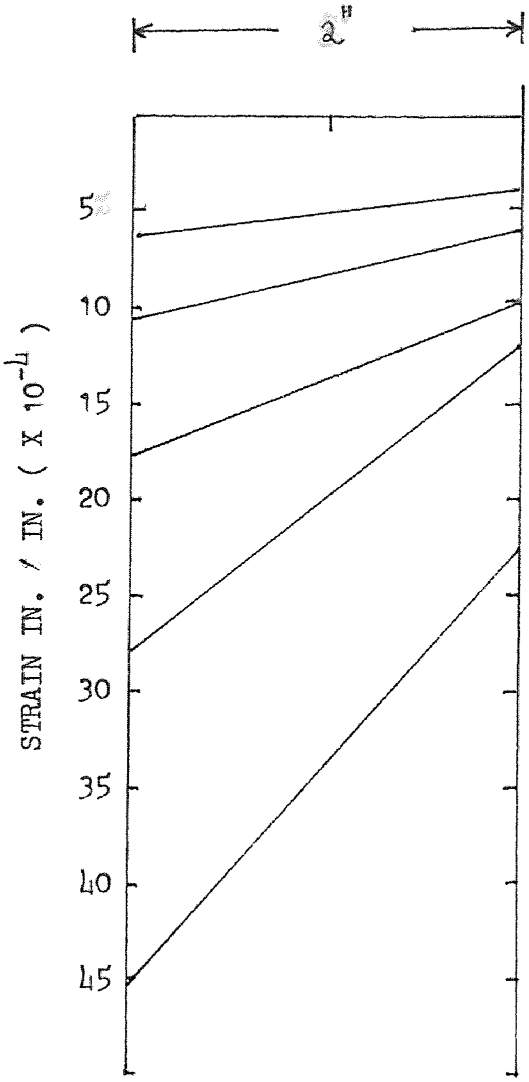

Fig. 5.6 STRAIN DISTRIBUTION LEADING TO ϕ_x
COLUMN #4

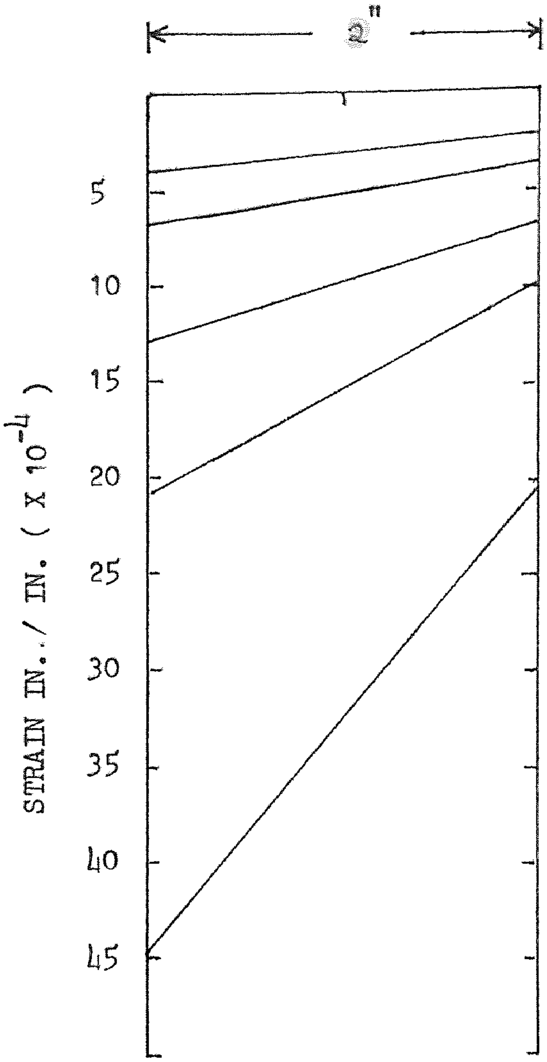

Fig. 5.7 STRAIN DISTRIBUTION LEADING TO ϕ_y
COLUMN #4

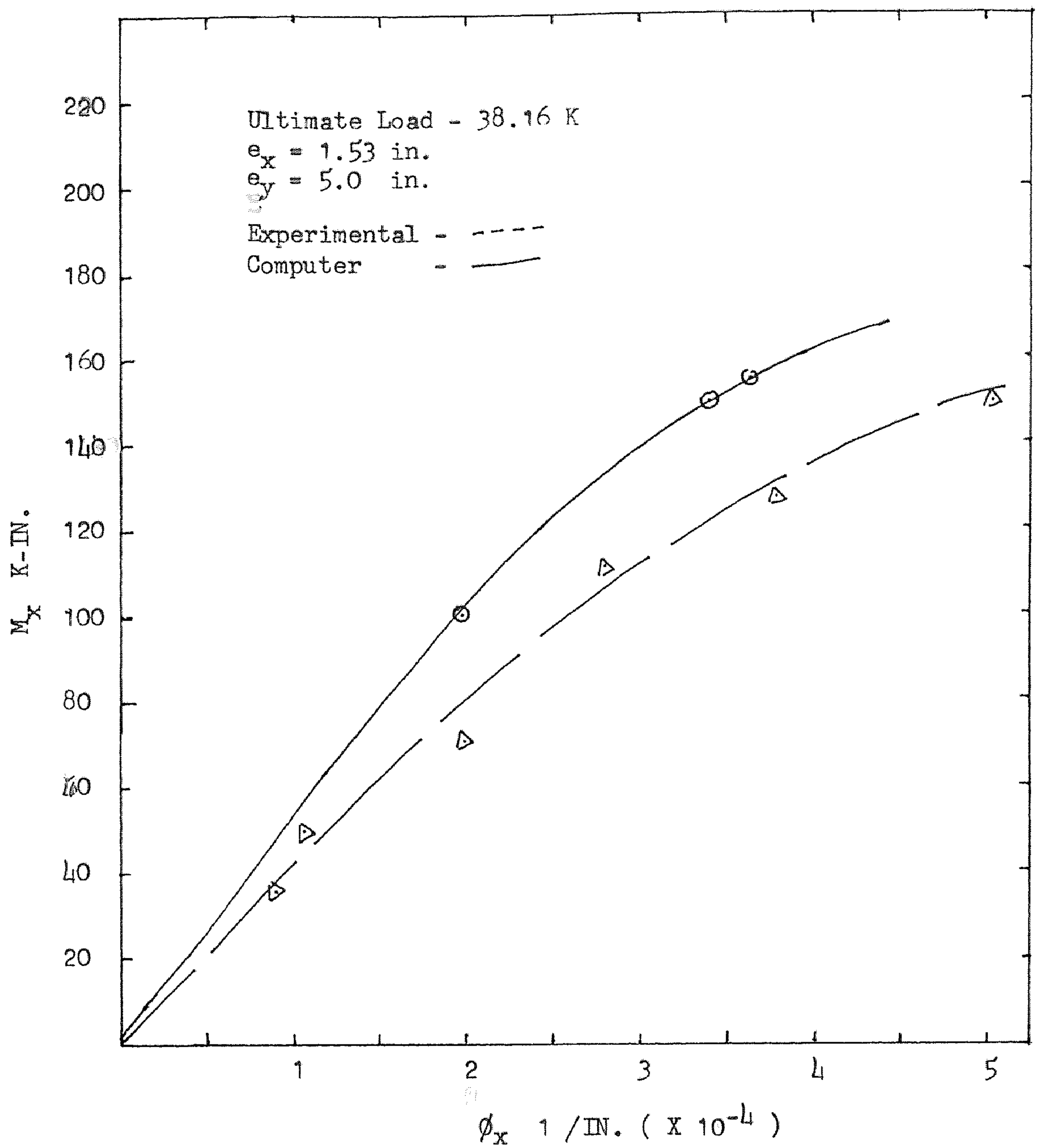

Fig.-5.8 M_x-ϕ_x CURVE FOR COLUMN #2

XP - XW
2 # 107

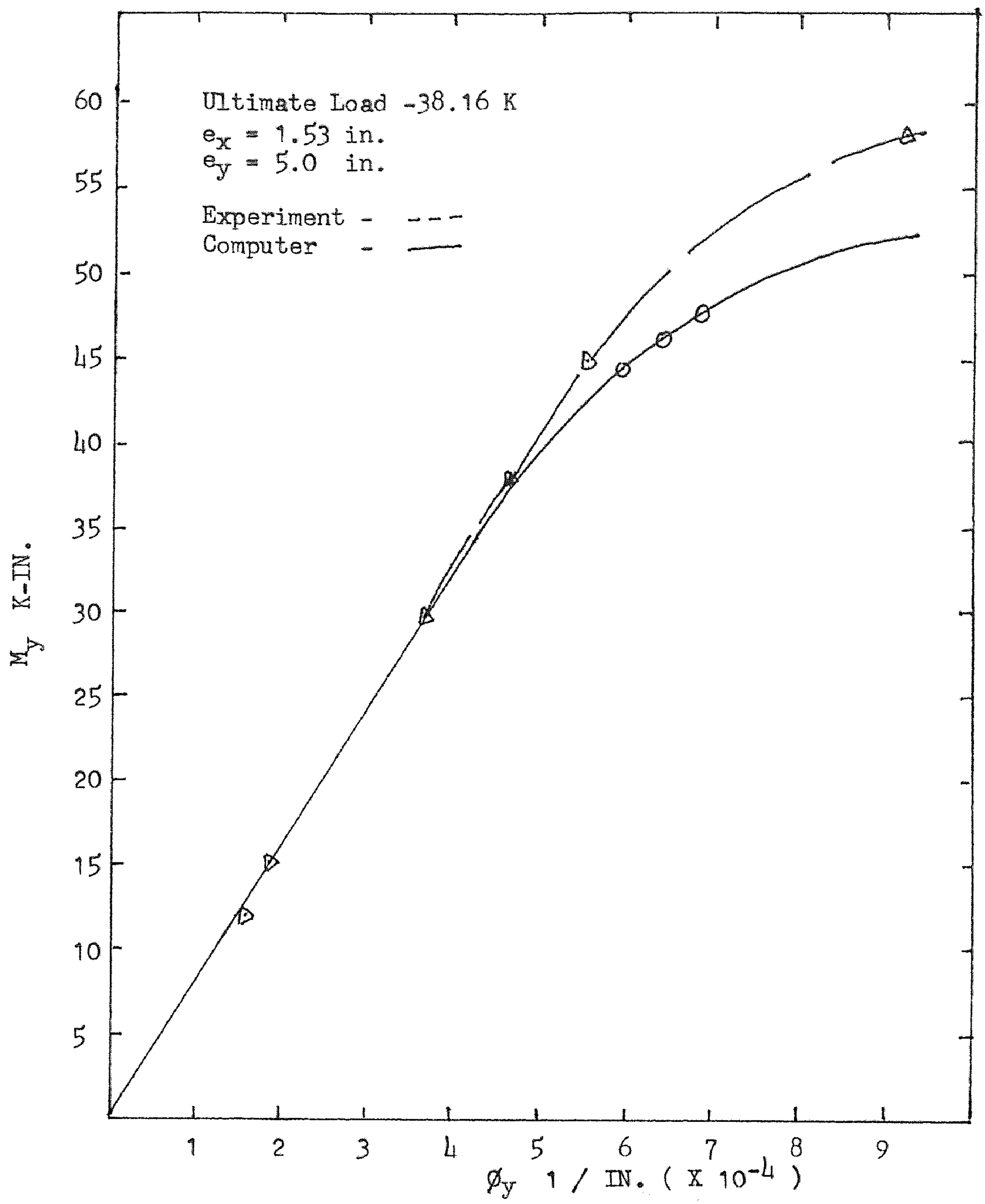

Fig. 5.9 M_y - ϕ_y CURVE FOR COLUMN #2

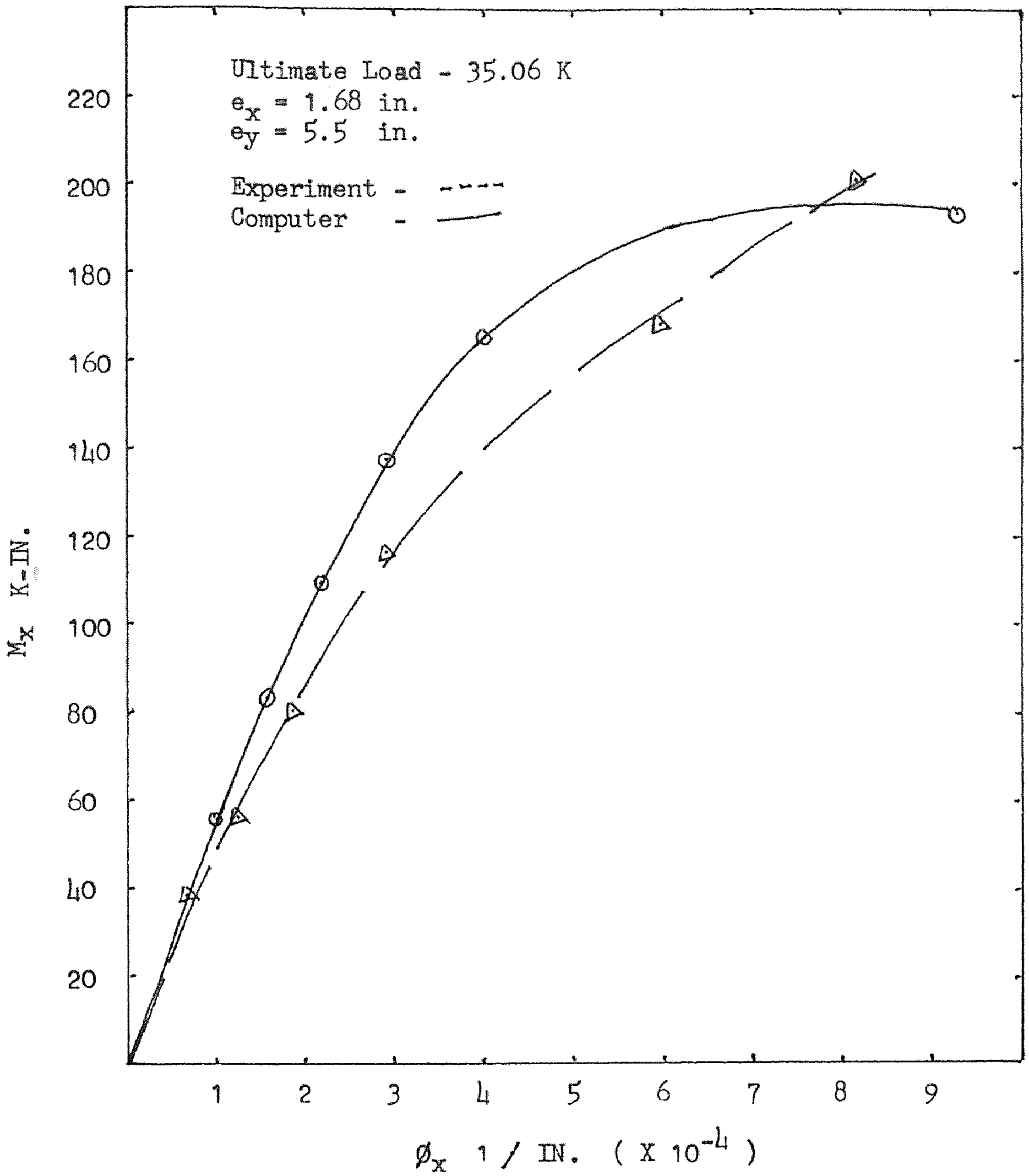

Fig. - 5.10 M_x - ϕ_x CURVE FOR COLUMN #3

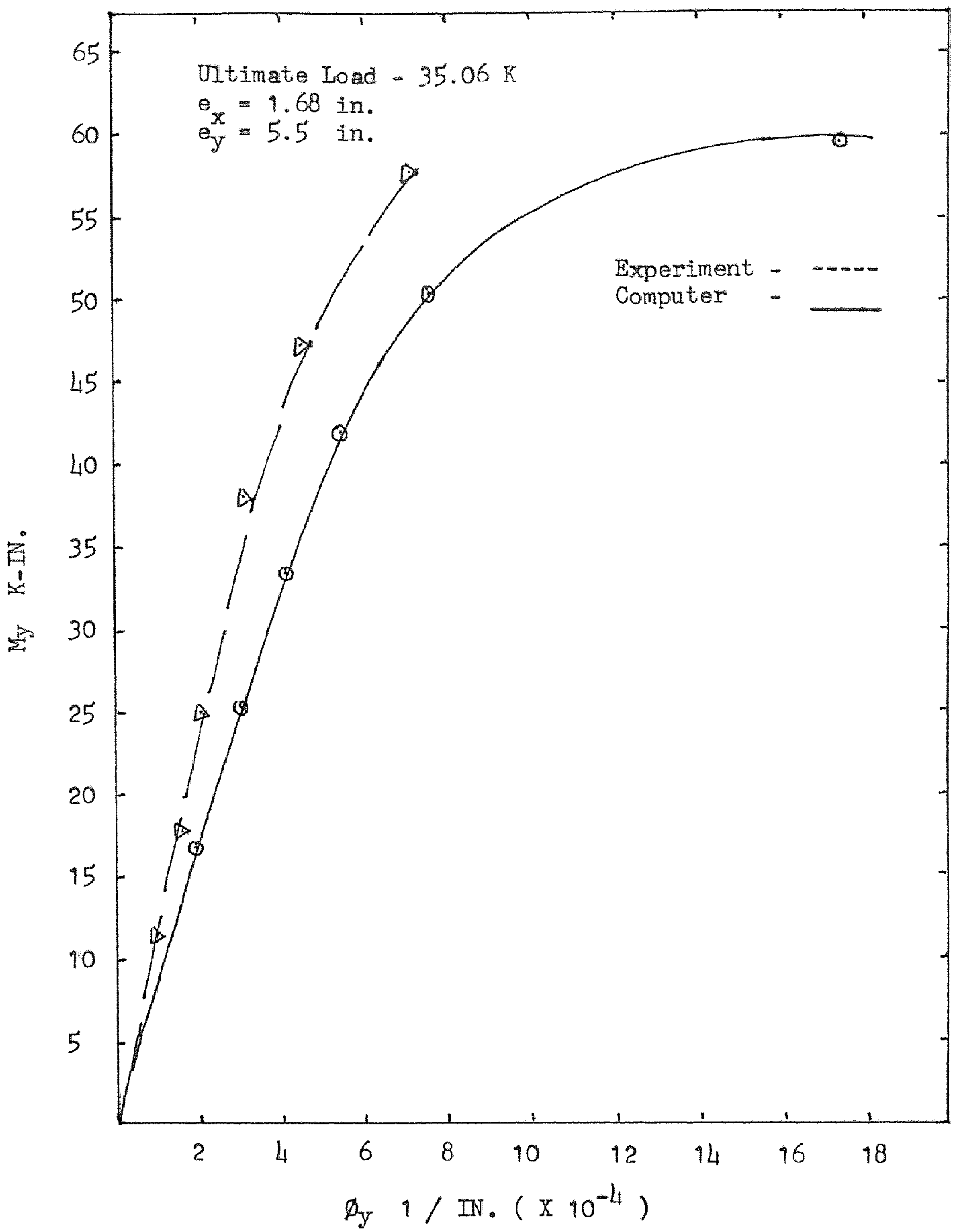

Fig. - 5.11 M_y - ϕ_y CURVE FOR COLUMN #3

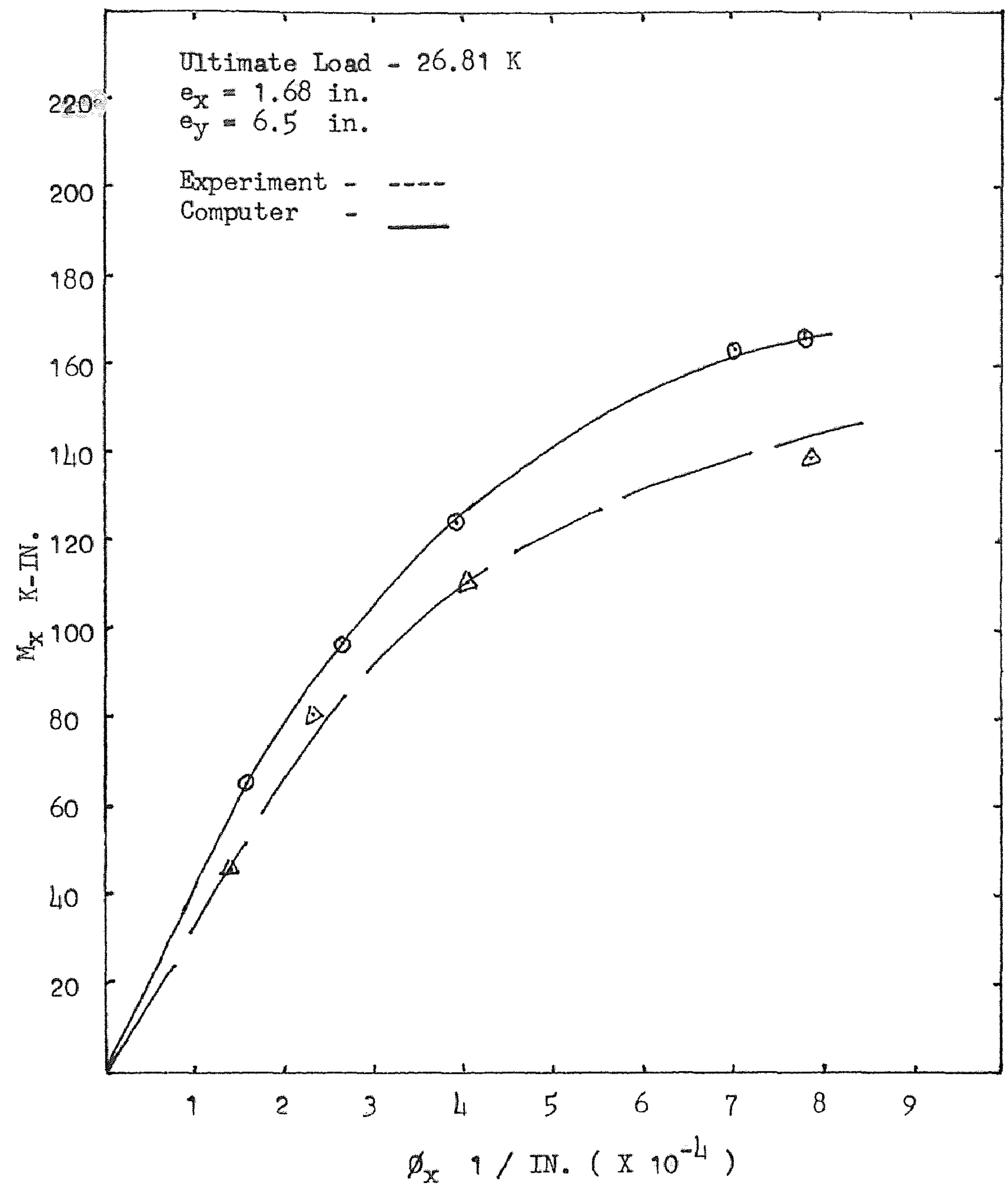

Fig. - 5.12 M_x - ϕ_x CURVE FOR COLUMN #4

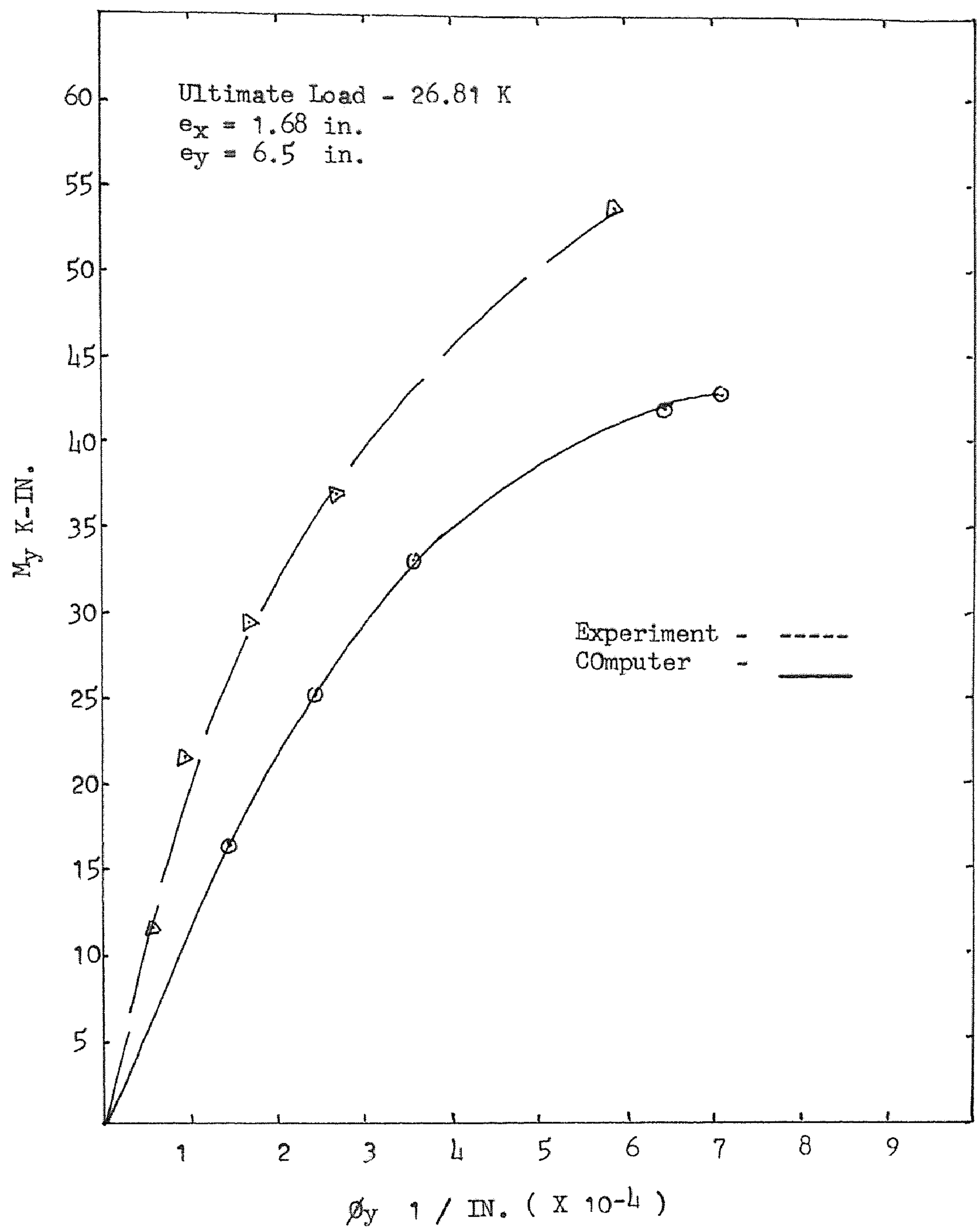

Fig. - 5.13 M_y - ϕ_y CURVE FOR COLUMN #4

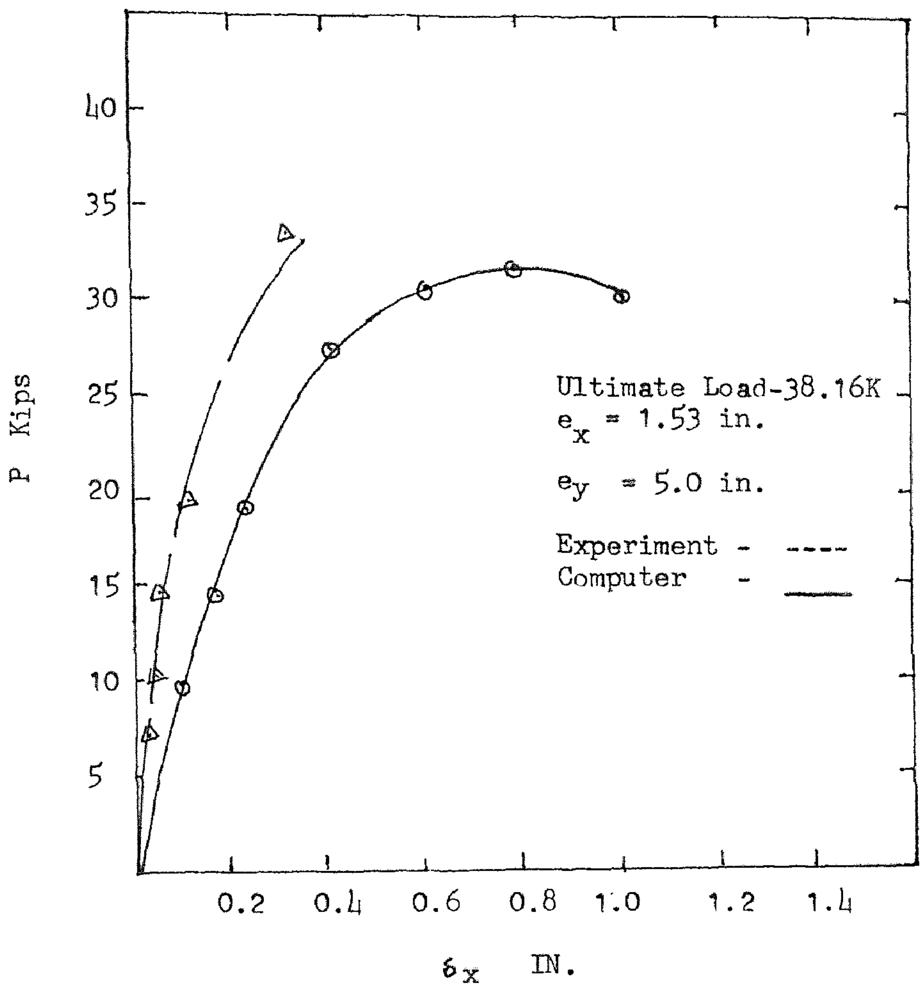

Fig. - 5.14 P - δ_x COLUMN #2

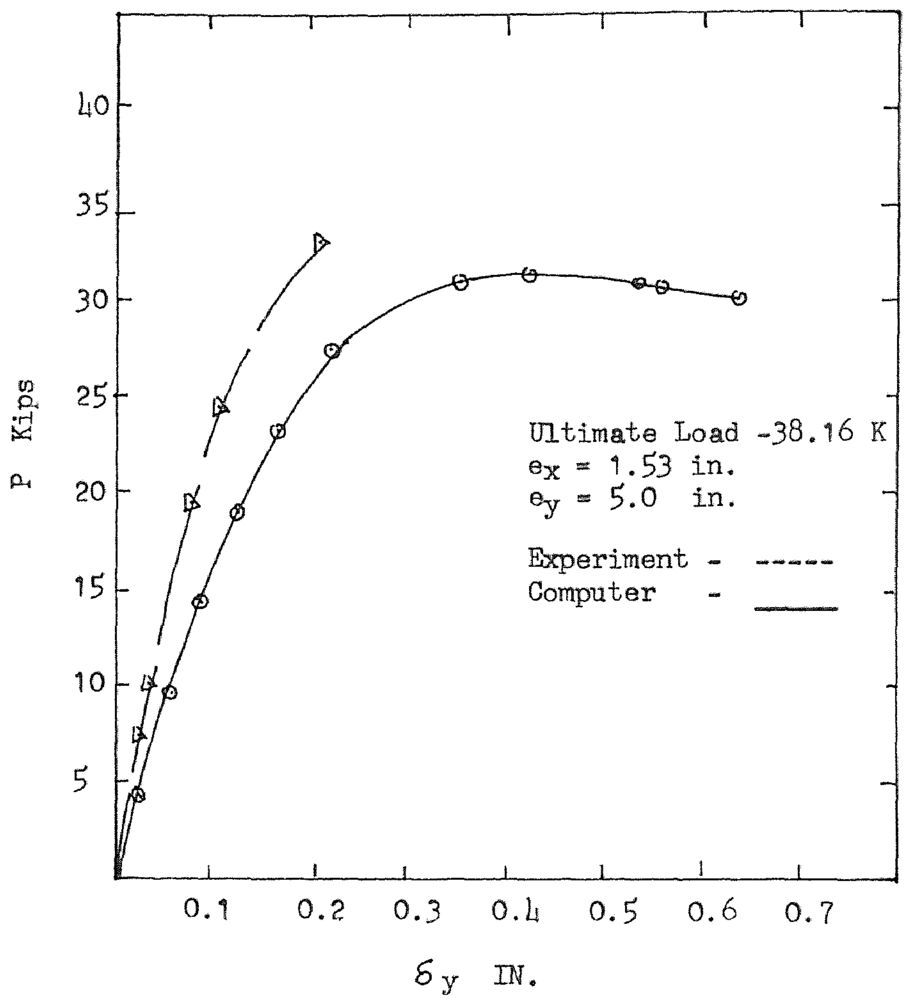

Fig. 5.15 P - δ_y CURVE FOR COLUMN #2

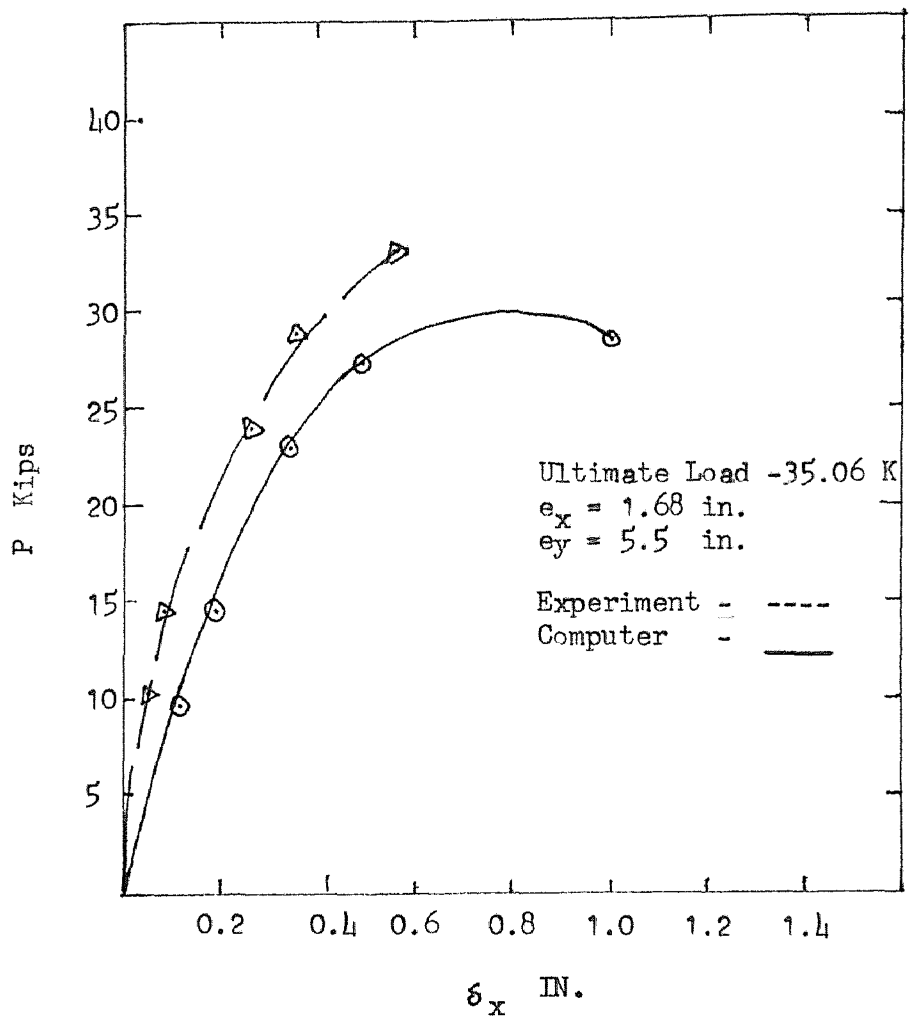

Fig. - 5.16 P - δ_x CURVE FOR COLUMN #3

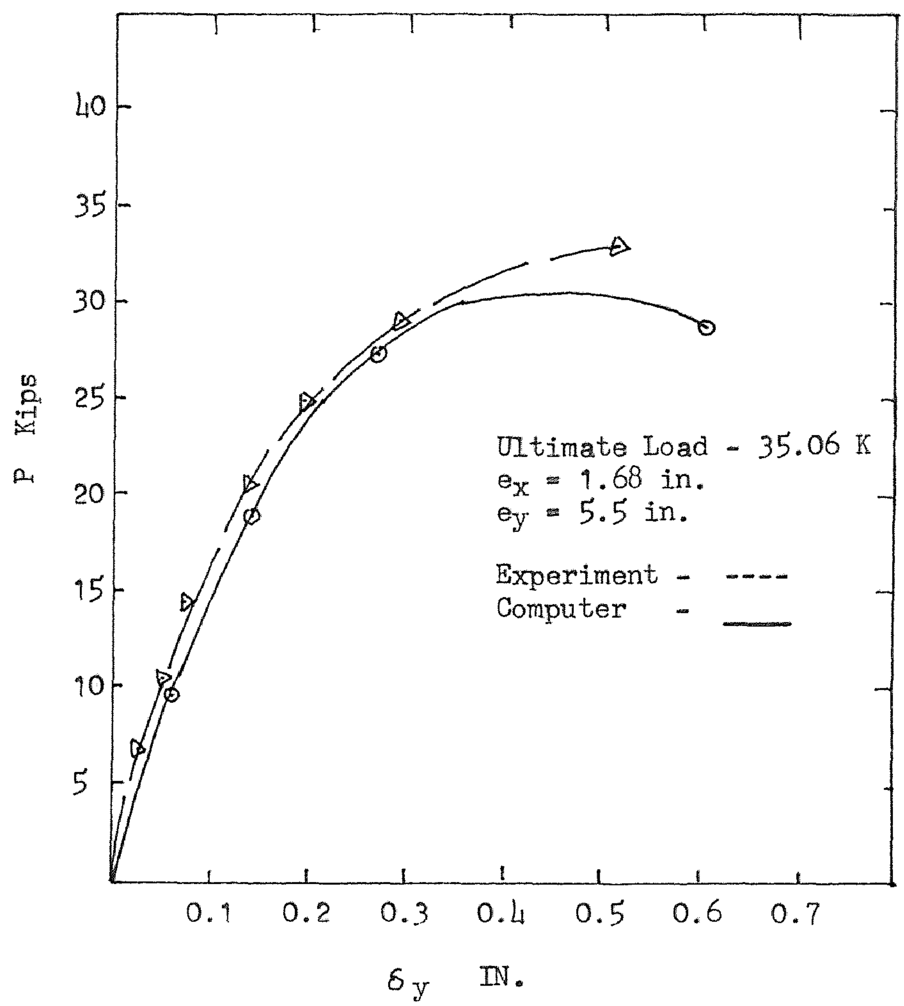

Fig. - 5.17 P - δ_y CURVE FOR COLUMN #3

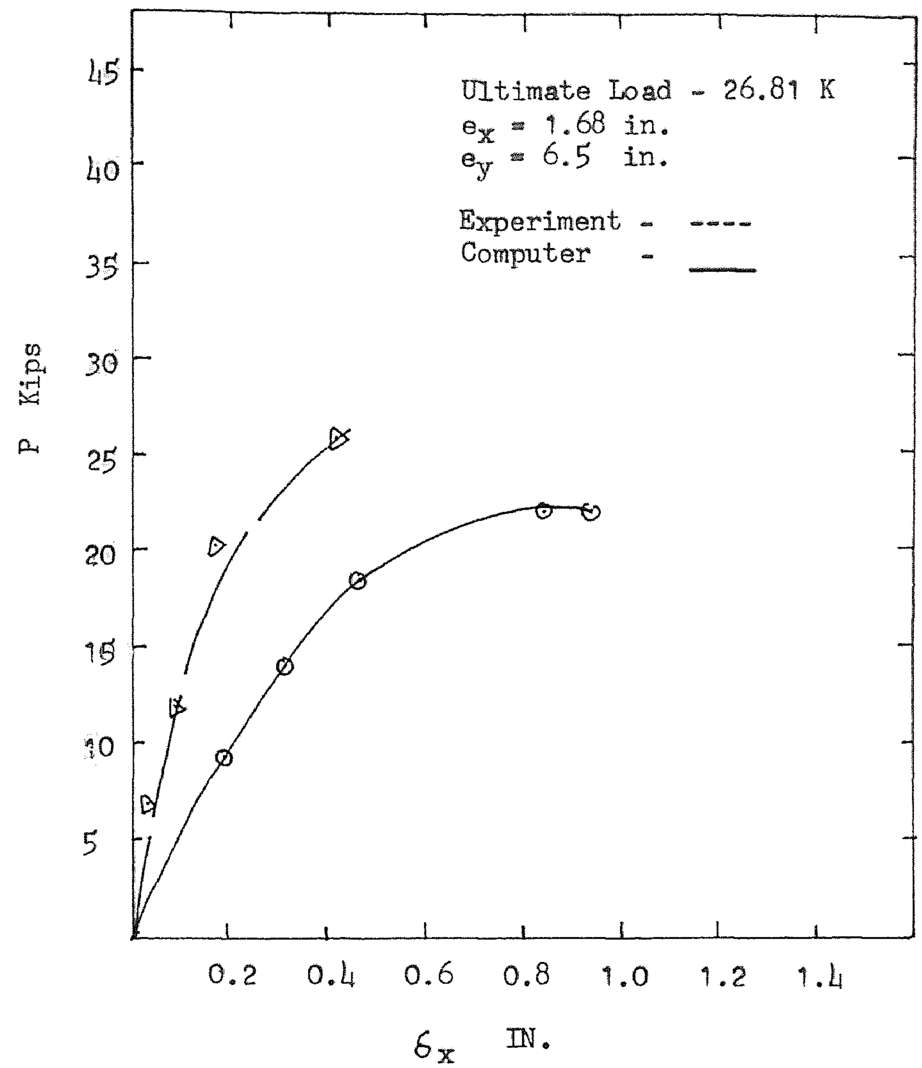

Fig. - 5.18 P - δ_x CURVE FOR #4

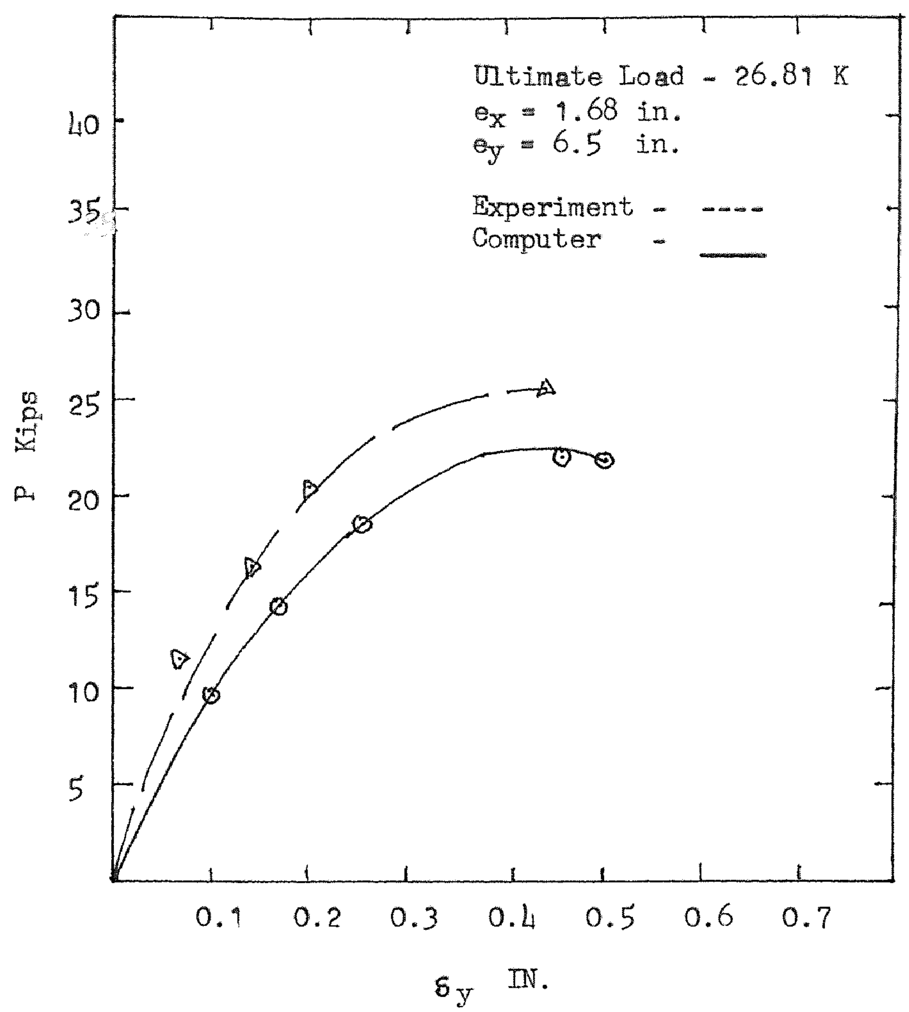

Fig. -5.19 P - δ_y CURVE FOR COLUMN #4

CHAPTER VI

COMPARATIVE STUDY AND DISCUSSION

Since the ultimate load, $M_x-\phi_x$, $M_y-\phi_y$ and $P-\delta$ curves are of primary intrest, in this chapter the writer concentrates on the discussion and the comparative study of the experimental and the computer results for the same.

1. As seen in the experimental $M-\phi$ curves, final rupture of the specimens were preceded by rapid, large curvature increase.

2. After the maximum moment was attained, the measured $P-M-\phi$ relationships differed significantly from those calculated using commonly accepted concrete stress-strain curves with strain limits of 0.003 in. / in.

3. In comparing $Mx-\phi_x$ curves there was a good agreement except the theoretical curves show more ductility of the specimens than indicated by the test results. This behavior might be attributed to the load controlled test procedure.

4. In comparing $My-\phi_y$ curves there was extremely

good agreement. Experimental $M_y - \phi_y$ curves are well above the theoretical $M_y - \phi_y$ curves and show more ductility of the specimens than that of predicted by the computer results. Therefore it can be concluded that the computer program is on the conservative side.

5. For both the curves, $M_x - \phi x$, $M_y - \phi y$ a good agreement was found between the experimental and theoretical results for the first 70% of the load increments. As the load increased toward the failure, difference was larger.

6. The computer program accurately predicts the ultimate strength.

7. The theoretical and experimental curves do not coincide. This behavior might be attributed to the experimental errors and the fact that the measurements of the strain ditribution were done over a 3 in. range as shown in Fig. 3.3. In the previous study (see Ref. 16), the measurements of the strains were taken over a 6 and 7.5 in. ranges for X and Y directions respectively. Even then the difference between the experimental and the theoretical results is not much.

8. A few experimental load-deflection curves do not agree with the analytical curves. This might again be attributed to unavoidable experimental errors and the

fact that the deflections in both the directions could not be measured exactly at mid-height of the columns.

Table : 6.1

COMPARATIVE STUDY OF EXPERIMENTAL AND COMPUTER RESULTS

Col no.	f_c' Psi	e_x in.	e_y in.	P Expt. Kips	P Comp. Kips	M_x Expt. K-in. *	M_x Comp. K-in.	M_y Expt. K-in. *	M_y Comp K-in
2	4200	1.53	5.0	34.0	31.60	183.8	158.0	65.7	48.3
3	4200	1.68	5.5	35.06	35.02	210.8	192.3	78.3	58.8
4	4000	1.68	6.5	26.81	25.44	188.2	165.3	56.1	42.7

* -For calculation of the ultimate moments, M_x and M_y deflection at the loading stage before the collapse was considered.

CHAPTER VII

CONCLUSIONS

From the experimental and analytical results the following conclusions can be deduced.

1. Theoretical analysis (the computer program) accurately predicts the ultimate strength.

2. In general a good agreeement between the experimental P-M-ϕ and P-δ relations and those of analytical was found. Consequently it can be concluded that the computer program developed by Hsu(1) can be used to find the ultimate strength, the moment-deformational characteristics, the stress-strain distribution across the section and the interaction surface of L-shaped, short column loaded biaxially with large and small eccentricities.

3. The results of this investigation could be used to develop the strength interaction diagrams and the failure surfaces that are needed in determining the value of an exponent α that appears in the non-dimensional equation(1.1) suggested by Bresler(12).

4. Further research may be conducted to consider the

effects of length of the member, shape of the section, and the torsion for the analytical procedure of the computer program.

APPENDIX -1

X, Y-COORDINATES AND AREA OF ELEMENTS OF THE CROSS SECTION

Element No.	X Coordinate in.	Y Coordinate in.	Area $in.^2$
1.	2.189	-2.077	0.110
2.	1.506	-3.414	0.110
3.	0.171	-2.733	0.110
4.	-1.165	-2.052	0.110
5.	-2.502	-1.371	0.110
6.	-1.821	-0.003	0.110
7.	-1.140	1.302	0.110
8.	-0.459	2.639	0.110
9.	0.222	3.975	0.110
10.	1.559	3.294	0.110
11.	0.876	1.956	0.110
12.	0.197	0.621	0.110
13.	-0.484	-0.715	0.110
14.	0.852	-1.396	0.110
15.	2.189	-1.872	0.316
16.	2.602	-2.290	0.211

17.	2.394	-2.706	0.316
18.	2.136	-3.209	0.316
19.	1.925	-3.626	0.211
20.	1.713	-4.044	0.316
21.	1.295	-3.831	0.211
22.	0.877	-3.616	0.316
23.	0.376	-3.363	0.316
24.	-0.046	-3.150	0.211
25.	-0.046	-2.937	0.316
26.	-0.960	-2.682	0.316
27.	-1.378	-2.469	-0.211
28.	-1.796	-2.256	0.316
29.	-2.297	-2.001	0.316
30.	-2.715	-1.788	0.211
31.	-3.133	-1.575	0.316
32.	-2.920	-1.156	0.211
33.	-2707	-0.740	0.316
34.	-2.452	-0.239	0.316
35.	-2.239	0.179	0.211
36.	-2.026	0.597	0.316
37.	-1.771	1.096	0.316
38.	-1.558	1.515	0.211
39.	-1.345	1.933	0.316
40.	-1.09	2.434	0.316

41.	-0.877	2.852	0.211
42.	-0.664	3.270	0.316
43.	-0.409	3.771	0.316
44.	-0.196	4.188	0.211
45.	0.017	4.606	0.316
46.	0.435	4.393	0.211
47.	0.853	4.180	0.316
48.	1.354	3.920	0.316
49.	1.772	3.712	0.211
50.	2.189	3.499	0.316
51.	1.976	3.082	0.211
52.	1.764	2.664	0.316
53.	1.508	2.163	0.316
54.	1.295	1.740	0.211
55.	1.083	1.327	0.316
56.	0.827	0.826	0.316
57.	0.614	0.409	0.211
58.	0.402	-0.009	0.316
59.	0.146	-0.510	0.316
60,	0.647	-0.765	0.316
61.	1.065	-0.978	0.211
62.	1.483	-1.191	0.316
63.	1.984	-1.446	0.316
64.	2.402	-1.659	0.211

65.	1.976	-2.495	0.211
66.	1.721	-2.996	0.211
67.	1.090	-3.201	0.211
68.	0.590	-2.945	0.211
69.	-0.247	-2.520	0.211
70.	0.748	-2.264	0.211
71.	-1.583	-1.839	0.211
72.	-2.084	-1.583	0.211
73.	-2.289	-0.903	0.211
74.	-2.034	-0.452	0.211
75.	-1.608	0.384	0.211
76.	-1.353	0.885	0.211
77.	-0.927	1.720	0.211
78.	-0.672	2.221	0.211
79.	-0.246	3.057	0.211
80.	-0.009	3.558	0.211
81.	0.640	3.763	0.211
82.	1.141	3.567	0.211
83.	1.346	2.877	0.211
84.	1.091	2.376	0.211
85.	0.665	1.54	0.211
86.	0.410	1.039	0.211
87.	-0.016	0.204	0.211
88.	-0.271	-0.297	0.211

89.	-0.067	-0.928	0.211
90.	0.434	-1.183	0.211
91.	1.270	-1.609	0.211
92.	1.771	-1.864	0.211
93.	1.556	-2.282	0.316
94.	1.303	-2.783	0.316
95.	0.802	-2.526	0.316
96.	0.384	-2.315	0.211
97.	0.034	-2.102	0.316
98.	-0.535	-1.897	0.316
99.	-0.952	-1.634	0.211
100.	-1.370	-1.421	0.211
101.	-1.871	-1.166	0.316
102.	-1.616	-0.665	0.316
103.	-1.403	-0.247	0.211
104.	-1.190	0.171	0.316
105.	-0.930	0.672	0.316
106.	-0.722	1.090	0.211
107.	-0.509	1.507	0.316
108.	-0.254	2.008	0.316
109.	-0.041	2.426	0.211
110.	0.172	2.844	0.316
111.	0.427	3.345	0.316
112.	0.928	3.090	0.316

113.	0.673	2.584	0.316
114.	0.460	2.171	0.211
115.	0.247	1.753	0.316
116.	-0.006	1.252	0.316
117.	-0.221	0.834	0.211
118.	-0.433	0.417	0.316
119.	-0.689	-0.084	0.316
120.	-0.902	-0.502	0.211
121.	-1.115	-0.920	0.316
122.	-0.697	-1.133	0.211
123.	-0.279	-1.346	0.316
124.	0.221	-1.601	0.316
125.	0.639	-1.814	0.211
126.	1.057	-2.027	0.316

SELECTED BIBLIOGRAPHY

1. Hsu, C.T.T., "Behavior of Structural Concrete Subjected to Biaxial Flexure and Axial Compression Ph.D. Thesis, M Gill University Aug., 1974.

2. Marin Joaquin. "Design Aids for L-shaped Reinforced Concrete Column", ACI Journal, Proceedings V. 76, No.6, November, 1979, pp. 1197-1215.

3. Ford, D.C. Chang and J.E. Breen. "Behavior of Concrete Columns under controlled lateral deformation", ACI Journal, Proceedings V. 78 Jan.-Feb. 1981, pp. 3-19.

4. Kurt H. Gerstle. "Simple Formulation of Biaxial Concrete Behavior", ACI Journal Proceedings V. 78, Jan.-Feb. 1981. pp. 62-68.

5. Richard W. Furlong. "Concrete Columns under Biaxially Eccentric Thurst", Journal of ACI, V. 76, Oct., 1979, pp.1093-1117.

6. Farah, A., and Huggins, M.M. "Analysis of Reinforced Concrete Columns Subjected to Longitudinal Load and Biaxial Bending", ACI Journal, V. 66, No. 7, July, 1969, pp.569-575.

7. Drysdale, R.G., and Huggins, M.M., "Size and Sustained Load Effects in Concrete Columns", Journal of Structural Division, ASCE, ST5, May, 1971, pp. 1423-1443.

8. Hognestad, E., "A Study of Combined Bending and Axial Load in Reinforced Concrete

   Members", Bulletin No. 399, Engineering Experiment Station, university of Illinois, Urbana, 1951, 128 pp.

9. ACI Committee 318, "Building Code requirements for Reinforced Concrete (ACI 318-77)".

10. C.K. Wang and Charles Salmon, "Reinforced Concrete Design", 3rd Edition, (New Yourk : Harper and Row Publisher, 1979), pp.451-469.

11. Robert, Park and T. Paulay, "Reinforced Concrete Structures", (New Yourk: John Wiley and Sons, 1975), pp. 133-135.

12. Boris Bresler, "Design Criteria for Reinforced Concrete Columns under Axial Load and Biaxial Bending", ACI Journal, Proceedings, 57, November 1960, pp.481-490.

13. F.N. Panell, "Failure Surfaces for Members in Compression and Biaxial Bending ", ACI Journal, Proceedings, 60, Jan., 1963, pp. 129-140.

14. L.N. Ramamurthy, "Investigation of Ultimate Strength of Square and rectangular Columns under Biaxially Eccentric Loads", Symposium on Reinforced Concrete Columns (SP-13), Detroit: ACI, 1966, pp.263-298.

15. Cheng-Tzu Thomas Hsu, "L-shaped Reinforced Concrete Column Section", Proceedings of the ASCE Engineering mechanics Speciality Conference, West Lafayette, Indiana, May 23-25, 1983.

16. C.T.T. Hsu, M.R. Tashehchian and M. Yeckta, "Inelastic Behavior of L-shaped Reinforced Concrete Columns", Proceedings of 9th Canadian Congress of Applied Mechanics, Saskatoon, Canada, May 30-June 3, 1983.

17. J.L. Meek, "Ultimate Strength of Columns with Biaxially Eccentric Loads", ACI Journal, Proceedings, 60, Aug., 1963, pp.1053-1064.

18. Dureseti Chidambarrao "Behavior of Channel-Shaped Reinforced Concrete Columns under Combined Biaxial Bending and Compression." Unpublished M.S. Thesis, NJIT, Sept. 1983.

19. W.B. Cranston, "A Computer Method for the Analsis of Reinforced Concrete Columns",

Cement and Concrete Association, London, Report TRA/402, April 1967.

20. Mon-Chen Liu, "Failure Surface for L-shaped Reinforced Concrete Short Column", Unpublished M.S. Thesis, NJIT, May 1983.

21. Cheng-Tzu Hsu and M.S. Mirza, "An Experimental-Analytical Study of Complete Load-Deformation Characteristics of Concrete Compression Members Subjected to biaxial Bending", Preliminary Report, International Association of Bridge and Structural Engineering, V. 16, Aug. 1974,PP 45-52.

22. T.A.Hafeez Khan and L.N. Ramamurthy "L-shaped Column Design for Biaxial Eccentricity", ASCE Journal of Structural Engineering, V. 109, No. 8, Aug., 1983.

23. Anderson, P. and Lee, H.N. "A Modified Plastic Theory of Reinforced Concrete", Bulletin No.33, University of Minnesota, V. LIV, No. 19, April, 1951.

24. Timosenko, S. and McCullough, G.H. "Elements of Strength of Materials", Third Edition, D. Van Nostrand Company, Inc., Princeton, NJ. May 1959.

25. Mattock, A.H. "Limit Design for Structural Concrete", Portland Cement Association Research and Development Lab., V. 1, No.2, Bulletin D38, May 1959.